Aspects of Molecular Medicine 3 (2024) 100033

Contents lists available at ScienceDirect

Aspects of Molecular Medicine

journal homepage: www.journals.elsevier.com/aspects-of-molecular-medicine

Human serum albumin binds spike protein and protects cells from SARS-CoV-2 infection by modulating the RAS pathway

Romualdo Varricchio [a,1], Giovanna De Simone [a,1], Gian Marco Vita [a], Walter Nocera Cariola [a], Maurizio Viscardi [b], Sergio Brandi [b], Gerardo Picazio [b], Verena Zerbato [c], Raffaella Koncan [d,e], Ludovica Segat [d], Stefano Di Bella [e], Giovanna Fusco [b], Paolo Ascenzi [a], Alessandra di Masi [a,*]

[a] Department of Sciences, Section of Biomedical Sciences and Technologies, Roma Tre University, 00146 Roma, Italy
[b] Istituto Zooprofilattico Sperimentale del Mezzogiorno, 80055 Portici (NA), Italy
[c] Infectious Diseases Unit, Azienda Sanitaria Universitaria Giuliano Isontina (ASUGI), 34128 Trieste, Italy
[d] Unità Complessa Operativa Igiene e Sanità Pubblica, Azienda Sanitaria Universitaria Integrata Giuliano Isontina (ASUGI), Trieste, Italy
[e] Clinical Department of Medical, Surgical and Health Sciences, Trieste University, 34149 Trieste, Italy

ARTICLE INFO

Keywords:
ACE2
Human serum albumin
Renin-angiotensin pathway
SARS-CoV-2
S1 domain
Spike

ABSTRACT

Since the start of the pandemic, scientists have directed their research towards identifying COVID-19 risk factors and predictive elements. Numerous clinical studies have established a strong connection between hypoalbuminemia and an unfavorable prognosis for COVID-19. Here, we aim to explore the impact of human serum albumin (HSA) on SARS-CoV-2 infection. Our findings indicate that HSA plays a role in reducing the replication rate of SARS-CoV-2 in Vero E6 cells. This protective effect is due to HSA ability to bind to the S1 domain of the spike protein, effectively competing with ACE2. Moreover, we show that the protective role of HSA is dependent also on its ability to activate the protective axis within the RAS system pathway, which is responsible for inducing vasodilation and promoting anti-inflammatory, anti-fibrotic, and anti-apoptotic responses. In summary, the data presented in this study support the idea that reduced levels of circulating HSA in hypoalbuminemic patients may heighten their susceptibility to SARS-CoV-2 infection, as the spike protein is unhindered in its ability to bind to ACE2 and penetrate human cells. Besides, hypoalbuminemia exacerbates the imbalance of the RAS pathway towards the classical "detrimental" axis. This could potentially contribute to the increased severity and elevated mortality rate observed in individuals with low levels of circulating albumin.

1. Introduction

Severe acute respiratory syndrome coronavirus 2 (SARS-CoV-2) is the causative agent of coronavirus disease 2019 (COVID-19), an atypical viral pneumonia first reported in December 2019 in Wuhan (China) (Zhu et al., 2020). SARS-CoV-2 possesses a single-stranded positive-sense RNA genome of 29.9 kb, encoding 16 non-structural, 4 structural, and 6 accessory proteins (Gioia et al., 2020; Lu et al., 2020). The structural proteins of SARS-CoV-2, namely nucleocapsid (N), membrane (M), envelope (E), and spike (S), have been documented (Gioia et al., 2020; Lu et al., 2020; da Silva Torres et al., 2022).

The spike protein plays a pivotal role in SARS-CoV-2 entry into human cells and represents the primary target for both vaccines and antiviral drugs (Almehdi et al., 2021). Spike is a transmembrane glycoprotein that forms homotrimers on the viral envelope, consisting of two functional subunits: S1 and S2. The S1 subunit comprises a *N*-terminal domain (NTD) and a receptor binding domain (RBD), which is the main interaction site with the human receptor angiotensin-converting enzyme 2 (ACE2), allowing viral entry into host cells (Hoffmann et al., 2020; Lan et al., 2020; Yan et al., 2020; V Raghuvamsi et al., 2021; Kirtipal et al., 2022). The S2 subunit comprises the fusion peptide, heptad repeats 1 and 2, the central helix, the connector domain, the transmembrane domain, and the cytoplasmic tail domain (V Raghuvamsi et al., 2021; Walls et al., 2020; Wrapp et al., 2020).

Receptor recognition marks the initial step of viral infection and is a crucial determinant of host cell and tissue tropism. ACE2 serves as the membrane receptor for SARS-CoV-2, facilitating binding and entry into host cells through endocytosis or membrane fusion (Hoffmann et al., 2020; Ou et al., 2020; Wan et al., 2020). Upon SARS-CoV-2 infection,

* Corresponding author.
E-mail address: alessandra.dimasi@uniroma3.it (A. di Masi).
[1] These Authors contributed equally to this work.

https://doi.org/10.1016/j.amolm.2023.100033
Received 13 October 2023; Received in revised form 10 December 2023; Accepted 11 December 2023
Available online 14 December 2023

Abbreviations

ACE	angiotensin-converting enzyme
ACE2	angiotensin converting enzyme 2
AIRs	ambiguous interaction restraints
Ang I	angiotensin I
Ang II	angiotensin II
AT1	angiotensin II type 1 receptor
AT2	angiotensin II type 2 receptor
CPE	cytopathic effects
E	envelope
FBS	fetal bovine serum
hpi	hours post-infection
HSA	human serum albumin
M	membrane
MOI	multiplicity of infection
N	nucleocapsid
NTD	*N*-terminal domain
RAS	renin-angiotensin system
RBD	receptor binding domain
RBM	receptor-binding motif
RT-qPCR	reverse transcription-quantitative polymerase chain reaction
S	spike
S1	subunit 1 of spike
S2	subunit 2 of spike

ACE2 is internalized into the cytoplasm (Banu et al., 2020) and is widely expressed in various organs, particularly in the heart and kidneys (Kirtipal et al., 2022; Ni et al., 2020; Salamanna et al., 2020). Although ACE2 expression in the lungs is not particularly high, the lungs are the major organs infected by SARS-CoV-2 (Huang et al., 2020).

Since the beginning of the pandemic, scientists have focused their efforts on identifying COVID-19 risks and prognostic factors (Sambataro et al., 2020). Several clinical studies have correlated a significant decrease in human serum albumin (HSA) levels in plasma with poor COVID-19 prognosis, suggesting that hypoalbuminemia (HSA levels $<$ 3.5 g/dL) predisposes patients to a faster progression of SARS-CoV-2 infection and systemic complications (Huang et al., 2020; Kheir et al., 2021; Soetedjo et al., 2021; Sanson et al., 2023; Zekri-Nechar et al., 2022; Zerbato et al., 2022). Indeed, COVID-19 patients with hypoalbuminemia are 2.1 times more likely to have severe disease and 1.5 times more likely to be hospitalized than patients with normal albumin levels. This suggests that hypoalbuminemic patients are sicker, have a worse prognosis, and require longer treatment (Chen et al., 2021; Georgieva et al., 2023).Accordingly, hypoalbuminemic patients have a significanlty higher mortality rate than those with normal HSA levels (23.85% vs. 0.9%, respectively) (Chen et al., 2021). It has been reported that 89% of patients with HSA levels of 4 g/dL and 68% of patients with HSA levels between 3.5 and 3.99 g/dL at the time of admission have been discharged alive within 30 days of hospitalization. In contrast, patients with HSA levels of 2.5 g/dL had a 60 percent higher mortality rate within 30 days after admission (Zekri-Nechar et al., 2022). However, the underlying mechanism by which low HSA correlates with poor outcomes in COVID-19 is not fully understood. From a pathogenetic perspective, endothelial dysfunction plays a significant role in COVID-19 (Bakker et al., 2021). This process leads to the loss of integrity of the epithelial–endothelial barrier, allowing the passage of fluids and proteins, including HSA, from the intravascular to the extravascular compartments, contributing to hypoalbuminemia. Therefore, hypoalbuminemia may serve as an indicator of the severity of epithelial-endothelial damage in patients with COVID-19 (Wu et al., 2021).

In this study, we investigated the role of HSA in SARS-CoV-2 infection. Specifically, we analyzed the interaction between HSA and spike using a combined *in silico*, *in vitro*, and *ex vivo* approach. The results demonstrate that HSA negatively modulates the replication rate of SARS-CoV-2 in Vero E6 cells. This protective mechanism can be attributed to HSA ability to recognize the RBD of the spike protein, competing with ACE2 binding. Additionally, we have shown that HSA modulates the RAS system, counteracting the RAS imbalance promoted by SARS-CoV-2. Overall, the data reported here elucidate, at the molecular level, the correlation between hypoalbuminemia and the progression of COVID-19.

2. Materials and methods

2.1. Reagents

The recombinant S1 domain of spike (6 × His-tag-S1) (Merck KGaA, Darmstadt, Germany) was dissolved in Phosphate Buffer Saline (PBS; 1.37×10^{-1} M NaCl, 1.0×10^{-2} M phosphate, 2.7×10^{-3} M KCl; Merck KGaA) at pH 7.4 to obtain a stock solution of 6.5×10^{-4} M. The recombinant human ACE2 protein (Merck KGaA) was dissolved in water to obtain a stock solution of 3.0×10^{-6} M. Fatty acid- and globulin-free HSA (Merck KGaA) was dissolved in deionized water at a final concentration of 1.0×10^{-4} M. All commercial proteins were of reagent grade and used without further purification. HSA concentration was determined spectrophotometrically using the value of ε_{280nm}: 39310 M^{-1} cm^{-1} (Vita et al., 2020). The S1 domain of Spike, ACE2, and HSA were handled following the manufacturer's instruction and using established good laboratory practices under biosafety cabinets with installed HEPA filters to avoid lipid contamination. For *in vitro* experiments using cell lines, albumin was administered using Albital (200 g/L; Grifols, Barcelona, Spain) The following primary antibodies were used for Western blot and ELISA experiments: anti-ACE2 (rabbit polyclonal; Thermo Fisher Scientific, MA, USA); anti-HSA (rabbit polyclonal; Merck KGaA); anti-HSA (mouse monoclonal; Santa Cruz Biotechnology); anti-SARS-CoV-2-Spike (rabbit polyclonal; Merck KGaA); anti-β-Actin (mouse monoclonal; Santa Cruz Biotechnology); anti-6 × His-tag (mouse monoclonal; Santa Cruz Biotechnology). The goat anti-mouse IgG and goat anti-rabbit IgG secondary antibodies were purchased from Bio-Rad (Hercules, CA, USA).

2.2. Virus isolation and growth in vero E6 cells and HSA treatment

African green monkey kidney cells (Vero E6) were cultured in Dulbecco Modified Eagle Medium (DMEM) (Corning, New York, NY, USA) complemented with 10% foetal bovine serum (FBS), 100 IU/mL penicillin-streptomycin solution, and 2.0×10^{-3} M L-glutamine. Vero E6 cells were cultured and treated in Biosafety Level 3 (BLS-3) laboratories. The SARS-CoV-2 delta variant AY61 sub-lineage (Gisaid accession n. EPI_ISL_3770696) was isolated from a clinical sample using Vero E6 cells (Ogando et al., 2020), with a concentration of 5.6×10^6 copies/μL determined by reverse transcription-quantitative polymerase chain reaction (RT-qPCR) (Cardillo et al., 2021). The isolated virus was titered using the End-point Dilution Assay (TCID50/mL) according to Spearman–Kärber method. To test the propagation of SARS-CoV-2 delta variant AY61 sub-lineage, Vero E6 cells were seeded at a density of 1.0×10^6 cells/mL in 25 cm^2 flasks; after 24 h, the surnatant was discarded, and the cells monolayer was infected with 1 mL of 0.1 multiplicity of infection (MOI) virus solution. After 1 h incubation, cells were grown in DMEM complemented with 2% FBS for 12 h and then harvested. To evaluate the protective role of HSA towards SARS-CoV-2 delta variant

AY61 sub-lineage infection, two experiments were designed. In the first experiment, Vero E6 cells were pre-treated for 12 h with 1.5×10^{-4} M HSA (Albital; Grifols); after incubation, the supernatant was removed, and the monolayer was infected for 12 h with 0.1 MOI virus solution. In the second experiment, 1.5×10^{-4} M HSA was incubated with 0.1 MOI virus solution for 1 h at 37 °C in FBS-free DMEM and then added to Vero E6 cells. As control, Vero E6 cells were also treated with the only HSA (1.5×10^{-4} M). To detect virus-induced cytopathic effects (CPE), control and infected cells were analyzed every 24 h and up to 72 h post-infection (hpi) using an inverted microscope (5 × magnification, Axiovert 25 inverted miscoscope; Carl Zeiss, Oberkochen, Germany) together with AxioVision 4.8 software. After microscope analysis, both supernatants and cells were collected and resuspended in TRIzol (Ambion, Life Technologies, Carlsbad, CA, USA). The RNA extraction and purification was performed using the MVP_2Wash_200_Flex program of the KingFisher Flex purification system (Thermo Fisher Scientific), following manufacturer's instructions. Virus quantification was performed by copy number quantification by RT-qPCR, using the TaqPath COVID-19 CE-IVD RT-PCR kit (Thermo Fisher Scientific) approved by the World Health Organisation (WHO). Amplification and thermal profiles were performed according to the protocol described previously (Cardillo et al., 2021) The assay was conducted in triplicate and reproduced in two independent experiments.

2.3. Magnetic beads pull-down

Fifteen microliters of nickel magnetic beads (MagneHis Protein Purification System, Promega, Madison, WI, USA) were coated with 2 µg of 6 × His-tag-S1 and incubated for 15 min at room temperature (RT) in slow rotation. After washing with 1.0×10^{-1} M HEPES buffer pH 7.5 (Promega), different concentrations of HSA (1.0×10^{-6} M, and 1.0×10^{-5} M) were added to the beads and incubated 1.5 h at 37 °C in slow rotation. The unbound fraction was removed and beads were washed 3 times with 1.0×10^{-1} M HEPES buffer pH 7.5. Finally, the elution buffer containing imidazole (Promega) was used to detach proteins from the beads. The presence of HSA and spike in the elution fractions was revealed by Western blot.

2.4. Western blot

Cells were lysed in NP-40 buffer (2.0×10^{-2} M Tris-HCl pH 8.0, 1.37×10^{-1} M NaCl, 10% glycerol (v/v), 1% NP-40 (v/v), 1.0×10^{-2} M EDTA, 1.0×10^{-3} M DTT, 2.0×10^{-3} M PMSF, and protease inhibitors). Protein lysates were quantified using the Bradford assay (Bio-Rad, Hercules, CA, USA). Twenty micrograms of whole protein lysate were loaded on SDS-PAGE and transferred on polyvinylidene fluoride (PVDF) membrane (Bio-Rad). After blocking for 1 h at RT with 3% non-fat dry milk (Bio-Rad) dissolved in 0.1% Tween-20/TBS (w/v/v) (TTBS), membranes were incubated overnight (ON) at 4 °C with primary antibodies. After three washes in 0.1% TTBS, membranes were incubated for 1 h at RT with the secondary antibody. Proteins were visualized using the Clarity™ Western ECL substrate (Bio-Rad). Images were acquired with the ChemiDoc™ Imaging system (Bio-Rad) and protein levels were quantified using the Image Lab software (version 2.1.0.35.deb, Bio-Rad). Experiments were repeated at least three times.

2.5. ELISA

ELISA experiments were performed as previously reported (Vita et al., 2020). The amount of 6 × His-tag-S1 required to efficiently coat the wells of the ELISA plate (NUNC MaxiSorp™ flat-bottom; Thermo Fisher Scientific) was determined using concentrations ranging from 1.0×10^{-8} M to 5.2×10^{-8} M. Once determined the proper concentration, wells were coated ON at 4 °C with 2.6×10^{-8} M 6 × His-tag-S1, washed in PBS, and blocked in 3% non-fat dry milk dissolved in PBS/0.05% Tween-20 (v/v) (PBS/T) for 1 h at RT. Increasing concentrations of either HSA (ranging from 5.0×10^{-8} M to 5.0×10^{-5} M) or ACE2 (ranging from 1.25×10^{-9} M to 1.60×10^{-7} M) were added to the 6 × His-tag-S1 pre-coated wells and incubated 90 min at 37 °C. HSA or ACE2 bound to the 6 × His-tag-S1 were detected using either the anti-HSA or the anti-ACE2 rabbit polyclonal antibodies. Subsequently, 100 µL of tetramethylbenzidine (TMB; Merck KGaA) was added to each well, and absorbance was measured at 370 nm until reaction saturation using the Tecan Spark 10 M (Tecan, Männedorf, Switzerland). Finally, the reaction was blocked using HCl 0.1 N.

2.6. Displacement-based ELISA

The wells coated with 2.6×10^{-8} M of 6 × His-tag-S1 were first incubated with 2.6×10^{-8} M ACE2 (corresponding to the determined ${}^{ACE2}K_0$ value) for 90 min at 37 °C, and then incubated with three different concentrations of HSA (2.5×10^{-6} M, 2.5×10^{-5} M, and 5.0×10^{-5} M). Conversely, 6 × His-tag-S1 coated wells were first incubated with 2.2×10^{-6} M HSA (corresponding to the determined ${}^{HSA}K_0$ value) for 90 min at 37 °C, and then incubated with three different concentrations of ACE2 (2.6×10^{-8} M, 5.3×10^{-8} M, and 1.1×10^{-7} M). HSA or ACE2 bound to 6 × His-tag-S1 were detected as described above.

2.7. Determination of the dissociation equilibrium constants for HSA:S1 and ACE2:S1 complex formation

Values of the dissociation equilibrium constants for HSA binding to 6 × His-tag-S1 in the absence and presence of ACE2 (${}^{HSA}K_0$ and ${}^{HSA}K_{ACE2}$, respectively) were determined at pH 7.4 and 37 °C. The HSA concentration ranged between 5.0×10^{-8} M and 5.0×10^{-5} M, the S1 concentration was 2.6×10^{-8} M, and the ACE2 concentration was 2.6×10^{-8} M.

Values of the dissociation equilibrium constants for ACE2 binding to S1 in the absence and presence of HSA (${}^{ACE2}K_0$ and ${}^{ACE2}K_{HSA}$, respectively) were determined at pH 7.4 and 37 °C. The ACE2 concentration ranged between 1.25×10^{-9} M and 1.60×10^{-7} M, the S1 concentration was 2.6×10^{-8} M, and the HSA concentration was 2.2×10^{-6} M.

Values of ${}^{HSA}K_0$ and ${}^{ACE2}K_0$ were obtained according to eqn. (1):

$$\alpha = [A] / \ (K_0 + [A]) \tag{1}$$

where α is the molar fraction of HSA:S1 or ACE2:S1, [A] is the HSA or ACE2 concentration and K_0 is ${}^{HSA}K_0$ or ${}^{ACE2}K_0$, respectively.

Values of ${}^{HSA}K_{ACE2}$ and ${}^{ACE2}K_{HSA}$ were obtained according to eqns (2) and (3):

$$\alpha = [A] / \ (K_{app} + [A]) \tag{2}$$

$$\alpha = 1 - \left([A] / \ (K_{app} + [A])\right) K_{app} + [A])[A] / \tag{3}$$

where α is the molar fraction of HSA:S1 or ACE2:S1 in the presence of ACE2 and HSA, respectively, and K_{app} is ${}^{HSA}K_{ACE2}$ or ${}^{ACE2}K_{HSA}$, respectively.

Values of ${}^{HSA}K_{ACE2}$ and ${}^{ACE2}K_{HSA}$ were calculated from values of ${}^{HSA}K_0$ and ${}^{ACE2}K_0$ at fixed ACE2 and HSA concentration according to eqns (4) and (5):

$${}^{HSA}K_{ACE2} = \left(\left({}^{HSA}K_0 / {}^{ACE2}K_0\right) \times [ACE2]\right) + {}^{HSA}K_0 \tag{4}$$

$${}^{ACE2}K_{HSA} = \left(\left({}^{ACE2}K_0 / {}^{HSA}K_0\right) \times [HSA]\right) + {}^{ACE2}K_0 \tag{5}$$

2.8. Protein-protein docking

Docking simulations of HSA (PDB ID: 1AO6) (Sugio et al., 1999) binding to the S1 domain of Spike protein (PDB ID: 7N9T) (Sun et al., 2021) were performed using HADDOCK2.4 web portal (Honorato et al., 2021; van Zundert et al., 2016). HADDOCK2.4 needs the generation of an Ambiguous Interaction Restraints (AIRs) file for a manual run to

define the active and passive residues present at the interface of each molecule. These residues were defined by the CPORT (Consensus Prediction Of Residues in Transient complexes) bioinformatic predictor (https://alcazar.science.uu.nl/services/CPORT/) (de Vries and Bonvin, 2011). Finally, the docked HSA:S1 domain complex (HSA:S1) were submitted to PRODIGY webserver (PROtein binDIng enerGY predict) (https://wenmr.science.uu.nl/prodigy/) (Vangone and Bonvin, 2017; Xue et al., 2016) to determine the binding energies and the intermolecular contacts.

2.9. Cell lines, culture conditions, and treatments

A549 human lung carcinoma epithelial cells and HepG2 human hepatoma cells were cultured in DMEM (Corning) complemented with 10% FBS (Corning), 100 IU/mL penicillin-streptomycin solution, and 2.0×10^{-3} M L-glutamine (Merck KGaA). SH-SY5Y neuroblastoma cells were maintained in complemented DMEM medium supplemented with 1% (v/v) nonessential amino acids (Biochrome GmbH, Berlin, Germany), 1% (v/v) Hepes (Merck KGaA), 1% (v/v) sodium pyruvate (Corning). Cells were grown at 37 °C and 5% CO_2. To evaluate HSA role in modulating the RAS system, A549 and SH-SY5Y cells were seeded at a density of 1.2×10^6. After 24 h, cells were placed in FBS-free DMEM medium and treated with 1.5×10^{-4} M HSA (Albital; Grifols) (Vita et al., 2020). After 6 h and 24 h, cells were either pelleted for Western blot analysis or collected in TRIzoL Reagent (Thermo Fisher Scientific) for subsequent RNA extraction and PCR analyses.

2.10. Reverse transcription-quantitative polymerase chain reaction (RT-qPCR)

Total RNA was extracted from cells resuspended in TRIzoL Reagent following the manufacturer's instruction (Thermo Fisher Scientific). One microgram of RNA was reverse transcribed using the GoScript™ Reverse Transcription System (Promega). The levels of ACE2, ACE, AT1, AT2, and MAS transcripts were evaluated by RT-qPCR using the oligonucleotides pairs reported in Table 1. β-actin was used as houkeeping gene (Bosso et al., 2019). The amplifications were performed using the GoTaq® qPCR SYBR Master Mix (Promega) and the Rotor Gene RG-6000 Real-Time Thermocycler (Corbett Research, Qiagen GmbH), using the following thermal cycling conditions: 95 °C for 2 min followed by 40 cycles at 95 °C for 10 s and 60 °C for 40 s. The data were reported using the $2^{-\Delta\Delta Ct}$ method.

2.11. Peripheral blood mononuclear cell isolation from patients

Peripheral blood was collected from 9 COVID-19 patients with normoalbuminemia (HSA levels ≥3.5 g/dL on admission) and 7 COVID-19 patients with hypoalbuminemia (HSA levels <3.5 g/dL on admission). Peripheral blood mononuclear cells (PBMCs) were isolated following the standard Ficoll-Paque density gradient centrifugation (Böyum, 1968) and cryopreserved until Western blot analysis. Albumin levels were analyzed by standard laboratory techniques (Sanson et al., 2023). Two milliliters of defibrinated blood were diluted with an equal volume of sterile 0.9 % NaCl (v/v) solution and layered carefully over 2 mL of Ficoll-Paque PLUS (Merck KGaA) without intermixing. After a centrifugation of 30 min at 400 rpm at RT, lymphocytes, monocytes, and platelets were harvested from the interface between the Ficoll-Paque PLUS and the sample layers. This material was then centrifuged twice for 10 min at 1600 rpm in sterile 0.9% NaCl solution to wash lymphocytes and to remove platelets. The pelleted PBMCs were finally resuspended in 1 mL of cell freezing medium without albumin. All procedures performed in this study involving human participants were in accordance with the ethical standards of the national research committee and with the 1964 Helsinki Declaration and its later amendments or comparable ethical standard. This study was approved by the Regional Ethics Committee of Trieste University Hospital (No. 2020-OS-072).

Table 1
Forward (FW) and reverse (RV) primers used for RT-qPCR analyses.

Gene	Primer sequences
ACE	FW: 5′- TCCTGTTGGATATGGAAACCACCTA -3′ RV: 5' - GTGGCCATCACATTCGTCAGA - 3′
ACE2	FW: 5'-TGGGATGGAGTACCGACTGGA-3' RV: 5'-GCATATGCAACAGATGATCGGAAC-3'
AT1	FW: 5′-GGGCGCGGGTTTGATATTTG -3′ RV: 5' -TCAAATACACCTGGTGCCGA - 3′
AT2	FW: 5′- ATTGAAGGAGTGTGTTTAGGCA - 3′ RV: 5′-TAGTGGCAAGGGTGGAGTTG -3′
MAS	FW: 5′-CCCAACTGAGGTTTCCATTGC-3′ RV: 5′-CAGGTAATTTTCTGGCAGTGACA- 3′
β-actin	FW. 5′-AGAGGGAAATCGTGCGTGAC-3′ RV: 5′-CAATGGTGATGACCTGGCCG-3′

2.12. Statistical analysis

Data were analyzed using GraphPad Prism 6 (GraphPad Software Inc., San Diego, CA, USA). All the experiments have been repeated at least three times. Data were expressed as mean values ± standard deviations (SD). Statistical analysis was performed using the Student's t-test or the One-way ANOVA test (*$p < 0.05$; **$p < 0.01$; ***$p < 0.001$; ****$p < 0.0001$).

3. Results

3.1. HSA decreases the viral replication rate of SARS-CoV-2

To evaluate the role of HSA in SARS-CoV-2 infectivity, Vero E6 cells were infected with 0.1 MOI of SARS-CoV-2 delta variant AY61 sublineage in the absence or presence of 1.5×10^{-4} HSA. The concentration of HSA used was chosen of the basis of previous data (Vita et al., 2020; di Masi et al., 2018) and based on preliminary experiments (data not reported). According to Araujo and coworkers (Araujo et al., 2020), the quantification of RNA copy number (RNAcn) by RT-qPCR indicated that the virus was released into the supernatant in a time-dependent manner, with RNAcn values slightly higher at 72 hpi, both in Vero E6 cell lysates and supernatants (Fig. 1A). The results obtained indicated that HSA significantly affected SARS-CoV-2 replication, as it markedly reduced the RNAcn values in both the tested experimental conditions. Specifically, when Vero E6 cells were pre-incubated with 1.5×10^{-4} M HSA for 12 h and then infected with 0.1 MOI virus solution for additional 12 h, we observed a 17.6-fold reduction ($p < 0.01$) in RNAcn values in cell lysates and a 38.5-fold reduction ($p < 0.01$) in the supernatants at 48 hpi, compared to infected Vero E6 cells (Fig. 1A). An even more pronounced protective effect was reported at 48 hpi when 0.1 MOI virus was pre-incubated with 1.5×10^{-4} M HSA for 1 h, and the mixture was then added to Vero E6 cells. In this case, we observed a 333-fold reduction ($p < 0.001$) in RNAcn values in cell lysates and a 100-fold reduction ($p < 0.001$) in the supernatants at 48 hpi, compared to infected Vero E6 cells (Fig. 1A). It is possible to hypothesize that infectivity increases after 72 h as HSA undergoes turnover, causing its levels in the medium to decrease over time.

3.2. HSA binds to the spike protein of SARS-CoV-2

A recent report suggests that the S1 subunit of the spike protein binds to native HSA (Zekri-Nechar et al., 2022). This binding capability decreases when HSA is glycated (Zekri-Nechar et al., 2022; Iles et al., 2022). Notably, in addition to hypoalbuminemia, hyperglycemia has also been reported as a risk factor for all-cause mortality in non-critically ill hospitalized COVID-19 patients (Carrasco-Sánchez et al., 2021). To elucidate the molecular basis of the protective effect of HSA against SARS-CoV-2 infection reported in Vero E6 cells (Fig. 1A), we initially sought to confirm the HSA:S1 interaction through pull-down

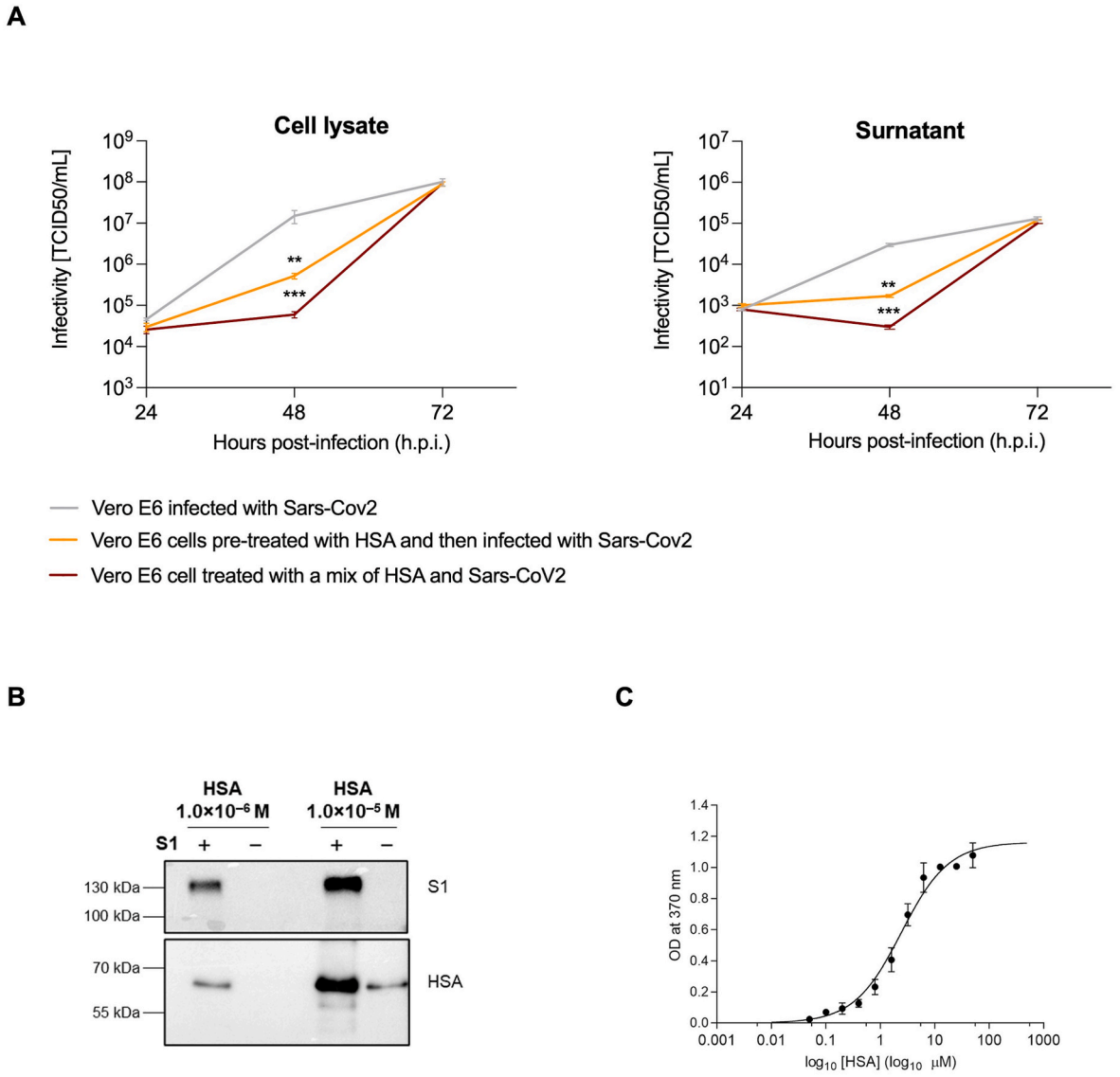

Fig. 1. HSA protect cells from SARS-CoV-2 infection and binds spike. (**A**) To test the propagation of SARS-CoV-2 delta variant AY61 sub-lineage, Vero E6 cells were infected with 0.1 MOI virus solution. After 1 h incubation, cells were grown in DMEM complemented with 2% FBS for further 12 h and then harvested. To evaluate the protective role of HSA towards SARS-CoV-2 delta variant AY61 sub-lineage infection, two experiments were designed. In the first experiment, Vero E6 cells were pre-treated for 12 h with 1.5×10^{-4} M HSA and then infected for 12 h with 0.1 MOI virus solution. In the second experiment, 1.5×10^{-4} M HSA was incubated with 0.1 MOI virus solution for 1 h at 37 °C in FBS-free DMEM and then added to Vero E6 cells. The quantification of RNA copy number (RNAcn) was performed by RT-qPCR in both cell lysates and supernatants. Data reported in the graphs indicate the means ± SD of three independent experiments (Student's t-test, $^{**}p < 0.01$, $^{***}p < 0.001$, with respect to Vero E6 infected cells in the absence of HSA). (**B**) S1 binding to HSA as evaluated by pull-down assay. Two different concentrations of HSA (1.0×10^{-6} and 1.0×10^{-5} M) were incubated with the 6 × His-tag-S1 coated (+) and uncoated (−) beads. Eluates were analyzed by immunoblot using the anti-HSA antibody. (**C**) S1 binding to HSA evaluated by ELISA. The relative dissociation constant was calculated (*i.e.*, $^{HSA}K_0 = (2.2 \pm 0.3) \times 10^{-6}$ M).

experiments. Using 6 × His-tagged S1 protein bound to Ni^{2+}-magnetic beads, we identified the HSA:S1 complex in the elution fractions using both anti-S1 and anti-HSA antibodies (Fig. 1B; Fig. S1). Notably, the formation of the HSA:S1 complex increased proportionally with the HSA concentration. Traces of HSA were detected at the highest concentration tested (*i.e.*, 1.0×10^{-5} M) in the beads without 6 × His-tagged S1, suggesting unspecific binding possibly due to the presence of short sequences of His residues in HSA.

S1 binding to HSA was determined also by ELISA, with the HSA concentration ranging from 5.0×10^{-8} M to 5.0×10^{-5} M in wells coated with 6 × His-tagged S1. The HSA-dependent increase in the absorbance at 370 nm allowed us to determine the apparent $^{HSA}K_0$ value, which was calculated as $(2.2 \pm 0.3) \times 10^{-6}$ M (Fig. 1C). The analysis of data according to eqn (1) indicated that the stoichiometry for HSA:S1 recognition was 1:1.

3.3. HSA competes with ACE2 in S1 recognition

To assess whether HSA and ACE2 compete for S1 binding, displacement-based ELISA assays were conducted (Fig. 2A and B). Initially, we added increasing concentrations of ACE2 (ranging from 1.25×10^{-9} M to 1.60×10^{-7} M) to wells coated with the 6 × His-tag-S1 protein to determine the $^{ACE2}K_0$ value, which was calculated as $(2.6 \pm 0.15) \times 10^{-8}$ M (Fig. S2). This value aligns with previously reported values ranging between 1.6×10^{-8} M and 1.2×10^{-7} M (Bayarri-Olmos et al., 2021; Huang et al., 2022; Yang et al., 2020). Subsequently, the 6 × His-tag-S1-coated wells were incubated with 2.6×10^{-8} M ACE2 and the ACE2:S1complex dissociation was evaluated by adding 2.5×10^{-6}

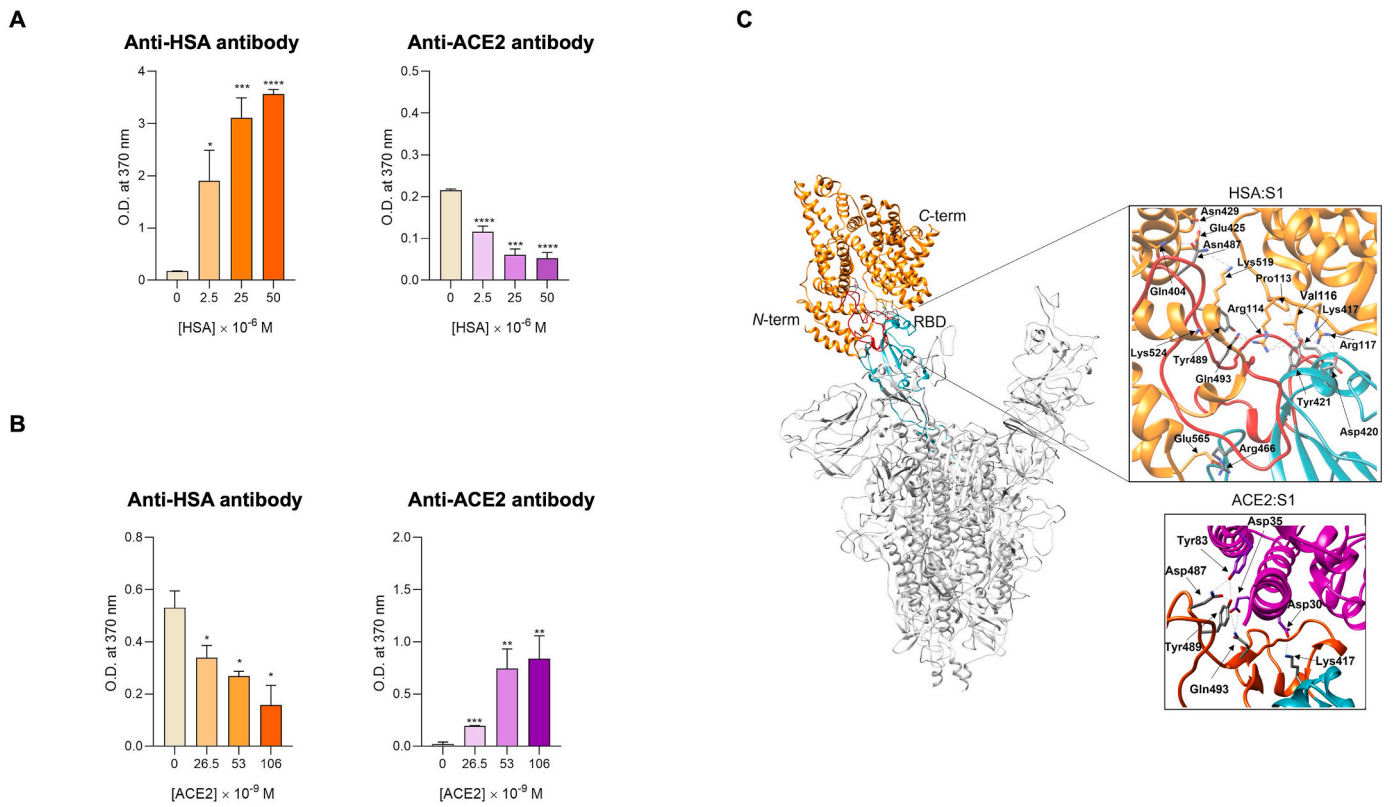

Fig. 2. HSA competes with ACE2 in S1 recognition. (**A**) To study the possible competition between HSA and ACE2 for the interaction with the S1 domain of spike, displacement-based ELISA was performed. Wells were coated with 2.6×10^{-8} M of 6 × His-tag-S1 and incubated with 2.6×10^{-8} ACE2 (corresponding to the determined K_d value) for 90 min at 37 °C. Wells were then incubated with three different concentrations of HSA (2.5×10^{-6} M, 2.5×10^{-5} M, and 5.0×10^{-5} M). The amount of HSA or ACE2 bound to 6 × His-tag-S1 were detected using either an anti-HSA (left) or an anti-ACE2 (right) primary antibody. (**B**) To confirm the competition, the displacement-based ELISA was further performed by coating wells with 2.6×10^{-8} M of 6 × His-tag-S1, followed by the incubation with 2.2×10^{-6} M HSA (corresponding to the determined K_d value) for 90 min at 37 °C. Wells were subsequently incubated with three different concentrations of ACE2 (2.6×10^{-8} M, 5.3×10^{-8} M, and 1.1×10^{-7} M). The amount of HSA or ACE2 bound to 6 × His-tag-S1 were detected using either an anti-HSA (left) or an anti-ACE2 (right) primary antibody (Student's t-test, *$p < 0.05$, **$p < 0.01$, ***$p < 0.001$, with respect to the control). (**C**) Molecular docking of the S1 domain of spike bound to HSA. Overall view of the putative complex between HSA (in orange) (PDB ID: 1AO6 (Sugio et al., 1999)) and the omo-trimeric spike (light grey) (PDB ID: 7N9T (Sun et al., 2021)). The boxes show the residues involved in HSA:S1 and ACE2:S1 interactions. Images were drawn with the UCSF Chimera-package (Pettersen et al., 2004). (For interpretation of the references to colour in this figure legend, the reader is referred to the Web version of this article.)

M, 2.5×10^{-5} M, and 5.0×10^{-5} M HSA. By adding antibodies directed against either HSA or ACE2, we observed a dose-dependent statistically significant increase in the fraction of HSA bound to the 6 × His-tag-S1-coated wells (Fig. 2A, left panel). Besides, a dose-dependent statistically significant decrease in the signal of the ACE2 fraction bound to the 6 × His-tag-S1-coated wells was observed (Fig. 2A, right panel).

To evaluate if reciprocal displacement occurs, the reverse experiment was conducted (Fig. 2B). Considering the ${}^{HSA}K_0$ value for HSA:S1 complex formation, calculated as $(2.2 \pm 0.3) \times 10^{-6}$ M, the 6 × His-tag-S1-coated wells were incubated with 2.2×10^{-6} M HSA and the HSA:S1 complex dissociation was evaluated by adding 2.6×10^{-8} M, 5.3×10^{-8} M, and 1.1×10^{-7} M of ACE2. Upon the addiction of ACE2, a dose-dependent statistically significant decrease in the fraction of HSA bound to the 6 × His-tag-S1-coated wells was observed (Fig. 2B, left panel), while a dose-dependent statistically significant increase in the ACE2 fraction was reported (Fig. 2B, right panel).

The analysis of data shown in Fig. 2, according to eqns (2) and (3), allowed to determine values ${}^{HSA}K_{ACE2}$ (=2.3×10^{-6} M and 7.7×10^{-6} M; Fig. S3A) and ${}^{ACE2}K_{HSA}$ (=4.7×10^{-8} M and 8.7×10^{-8} M; Fig. S3B) at fixed ACE2 (=2.6×10^{-8} M; Fig. S3A) and HSA (=2.2×10^{-6} M; Fig. S3B), respectively. To outline the competition of HSA and ACE2 for S1, values of ${}^{HSA}K_{ACE2}$ and ${}^{ACE2}K_{HSA}$ were calculated according to eqns (4) and (5) considering the following parameters ${}^{HSA}K_0$ (=2.2×10^{-6} M) and ${}^{ACE2}K_0$ (=2.6×10^{-8} M) at ACE2 = 2.6×10^{-8} M and HSA = 2.2×10^{-6} M. The calculated values of ${}^{HSA}K_{ACE2}$ (3.7×10^{-6} M) and ${}^{ACE2}K_{HSA}$ (3.8×10^{-8} M) agree with those obtained experimentally (Fig. S3).

To predict the HSA:S1 recognition region and to assess whether there are overlapping regions between HSA and ACE2 for the recognition of S1, molecular docking studies were performed. HSA is an all-α-helical protein arranged in three domains, namely domain I (amino acids 1–195), II (amino acids 196–383), and III (amino acids 384–585) (Fanali et al., 2012). The results here reported indicate that the binding interface between HSA and S1 is lined by Glu425, Asn429, Lys519, Lys524, Gln526, and Glu565 residues hosted in the domain III of HSA and by Arg466, Asn487, Tyr489, and Gln493 residues located in the RBM of S1. Furthermore, Pro113, Arg114, and Val116 residues placed in the domain I of HSA interfaces with Lys417 of S1. Finally, hydrogen bonds are established between Arg114, Arg117, and Lys524 residues placed in the domains I and III of HSA and Asp420, Tyr421, and Tyr489 residues located in the RBD of S1 (Fig. 2C). Of note, the Lys 417, Asn487, Tyr489, Gln493 residues of S1 also play a key role in ACE2 recognition (Figs. S4 and S5; Table S1) (Lan et al., 2020).

3.4. HSA modulates renin-angiotensin system pathway favoring the ACE2/Ang 1–7/MAS/AT2 axis

ACE2 functions as a counter-regulator of the renin-angiotensin system (RAS), which plays a crucial role in maintaining blood pressure, electrolyte balance, and fluid balance (Patel et al., 2017; Yang and Xu, 2017). The liver releases angiotensinogen, which is converted by plasma

renin into angiotensin I (Ang I). The angiotensin-converting enzyme (ACE), found on the surface of vascular endothelial cells, particularly in the lungs, transforms Ang I into angiotensin II (Ang II), which acts through the angiotensin II type 1 and type 2 receptors (AT1 and AT2, respectively) (Bian and Li, 2021). The ACE-Ang II-AT1 classical axis leads to vasoconstriction and increases blood pressure (Paz Ocaranza et al., 2020). Ang II is converted by ACE2 into the vasodilator Ang (1–7) or catalyzes Ang I conversion into Ang (1–9), which then ACE further cleaves into Ang (1–7) (Bian and Li, 2021). Ang (1–7) binds to the transmembrane MAS receptor, forming an ACE2-Ang (1–7)-MAS axis. It is generally assumed that the ACE2/Ang 1–7/MAS/AT2 pathway may counteract the effects of the classical RAS pathway, promoting anti-inflammatory, anti-hypertrophic, and anti-fibrotic effects, and it is therefore referred to as the "protective arm" of RAS (Yang and Xu, 2017; Bian and Li, 2021; Paz Ocaranza et al., 2020).

With the aim of identifying the molecular mechanism underlying the potential role of HSA in influencing COVID-19 progression, we explored the possibility that HSA could modulate the expression of RAS components (Fig. 3). Experiments were conducted using A549 adenocarcinomic human alveolar basal epithelial cells, SH-SY5Y neuroblastoma cells, and human hepatoma HepG2 cells. These cell lines serve as valuable models for studying respiratory virus infections and are characterized by the expression of RAS components (Huang et al., 2020; Wu et al., 2021; Bielarz et al., 2021). First, we investigated the ability of HSA to modulate the expression of the classical pathway of the RAS system, particularly focusing on ACE and AT1 transcripts. The results obtained indicated that HSA significantly induced, both after 6 and 24 h of treatment, the expression of ACE in A549 (1.3-fold, $p < 0.05$ at 6 h; 1.5-fold, $p < 0.01$ at 24 h) and HepG2 (2.3-fold, $p < 0.001$ at 6 h; 2.1-fold, $p < 0.01$) compared to untreated cells. In SH-SY5Y, ACE levels significantly increased only after 24 h (1.3-fold, $p < 0.01$) compared to untreated cells. Next, we examined the expression of AT1, which plays a key role in mediating the major cardiovascular effects of angiotensin II (Forrester et al., 2018). In this case, we observed an overall tendency of HSA to induce a downregulation of AT1 transcript. Specifically, in A549 and SH-SY5Y cells a statistically significant downregulation of AT1 was observed after 6 h (A549: 1.2-fold, $p < 0.05$; SH-SY5Y: 1.5-fold, $p < 0.05$) and 24 h (A549: 1.4-fold, $p < 0.01$; SH-SY5Y: 1.7-fold, $p < 0.05$) following HSA administration. In HepG2 cells, a slight downregulation was noted, although it was not statistically significant (Fig. 3).

In addition to the classical pathway of the RAS system, we examined the effect of HSA treatment on the ACE2/Ang 1–7/MAS/AT2 protective pathway. HSA induced an increase in ACE2 levels compared to controls (A549: 1.3-fold, $p < 0.05$ at 6 h, and 1.7-fold, $p < 0.01$ at 24 h; SH-SY5Y: 1.6-fold, $p < 0.05$ at 6 h, and 2.1-fold, $p < 0.01$ at 24 h; HepG2: 1.2-fold, $p < 0.05$ at 6 h). Besides, HSA also induced a significant increase of AT2 levels (A549: 1.3-fold, $p < 0.05$ at 6 h, and 2.4-fold, $p < 0.001$ at 24 h; SH-SY5Y: 1.5-fold, $p < 0.05$ at 6 h, and 1.7-fold, $p < 0.01$ at 24 h; HepG2: 1.4-fold, $p < 0.05$ at 6 h, and 1.7-fold, $p < 0.05$ at 24 h) (Fig. 3). On the contrary, MAS expression significantly increased in HSA-treated A549 (A549: 1.4-fold, $p < 0.05$ at 6 h, and 3.6-fold, $p < 0.001$ at 24 h; HepG2: 1.6-fold, $p < 0.05$ at 6 h, and 2.2-fold, $p < 0.01$ at 24 h). Conversely, in SH-SY5Y cells, MAS expression decreased following HSA treatment. Overall, data obtained indicate that HSA up-regulates the expression of the ACE2/Ang 1–7/MAS/AT2 receptor pathway, possibly promoting anti-inflammatory, anti-hypertrophic, and anti-fibrotic effects.

Next, we analyzed the modulation of the RAS pathway in Vero E6 cells infected for 48 h with 0.1 MOI of the SARS-CoV-2 delta variant AY61 sub-lineage, in the absence and presence of 1.5×10^{-4} M HSA (Fig. 4). First, we analyzed the response of Vero E6 cells to HSA treatment, which induced a significant increase in ACE, ACE2, AT2, and MAS levels compared to untreated cells (ACE: 2.4-fold, $p < 0.01$; ACE2: 2.4-fold, $p < 0.05$; AT2: 1.9-fold, $p < 0.5$; MAS: 2.3-fold, $p < 0.5$). According

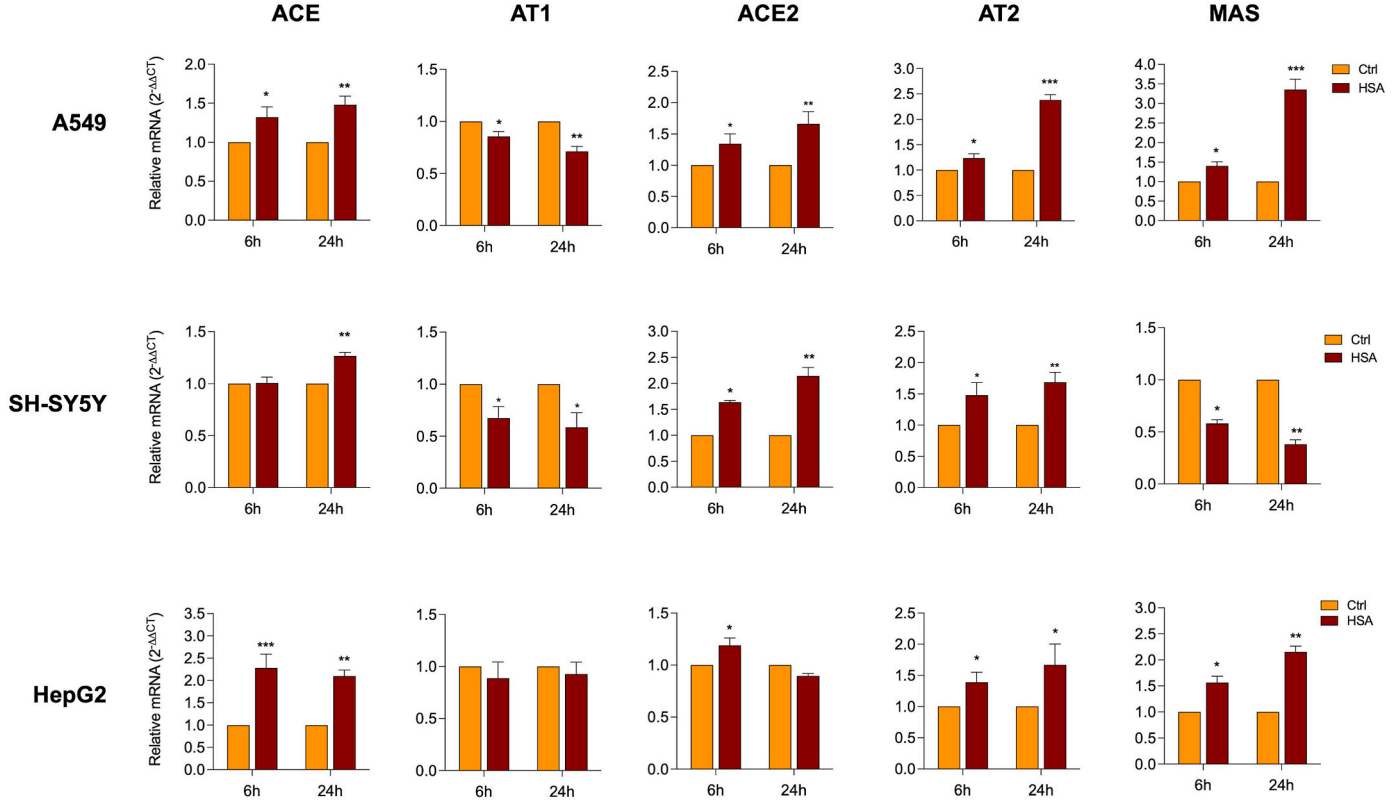

Fig. 3. HSA modulates the RAS system in A549, SH-SY5Y, and HepG2 human cells. Cells were treated with 1.5×10^{-4} M HSA for 6 and 24 h. Transcript levels of ACE, AT1, ACE2, AT2, and MAS were measured by RT-qPCR, normalized to α-actin, and reported using the $2^{-\Delta\Delta Ct}$ method. Data are reported as the mean ± SD of three independent experiments (Student's t-test, *$p < 0.05$; **$p < 0.01$; ***$p < 0.001$ with respect to the control).

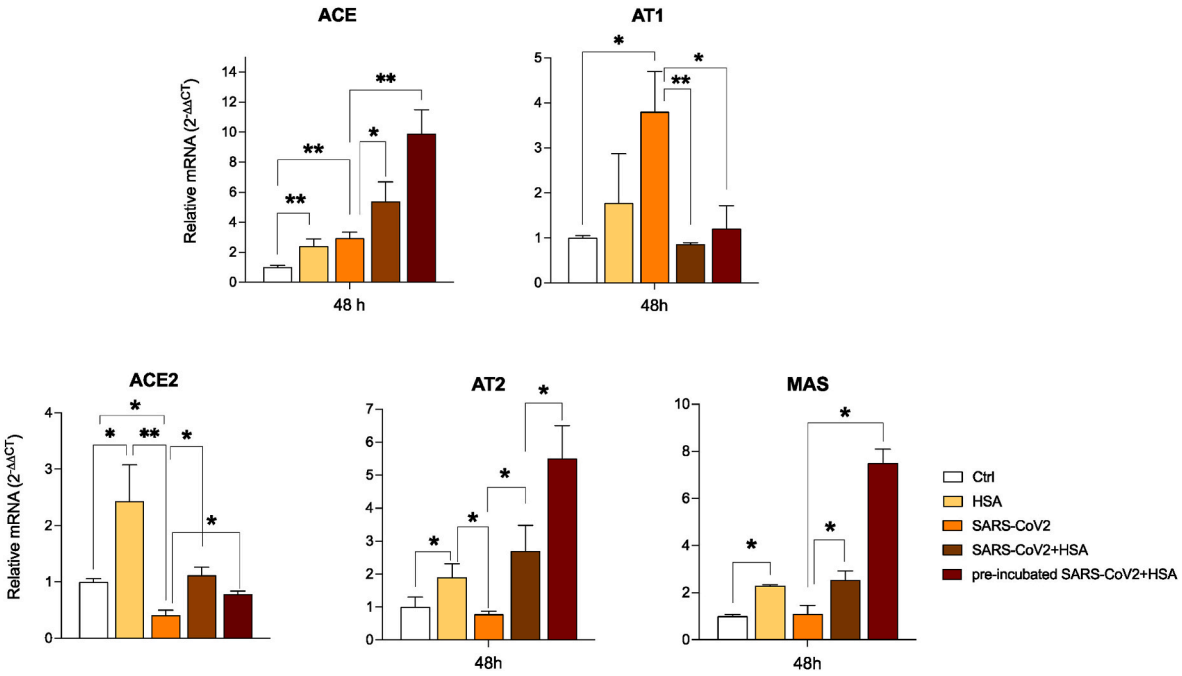

Fig. 4. HSA induces the transcriptional modulation of the RAS system in Vero E6 cells infected with SARS-Cov-2. Transcript levels of ACE, AT1, ACE2, AT2, and MAS were measured by RT-qPCR, normalized to α-actin, and reported using the $2^{-\Delta\Delta Ct}$ method. The graphs indicate the means ± SD of two different experiments (One-way ANOVA test, *$p < 0.05$, **$p < 0.01$).

to literature, when cells were infected with the SARS-CoV-2 virus, the ACE-AT1 classic pathway appeared to be activated compared to untreated cells (ACE: 2.9-fold; $p < 0.01$; AT1: 3.8-fold; $p < 0.05$). In contrast, the ACE2/Ang 1–7/MAS/AT2 pathway appeared to be suppressed, with ACE2 expression decreasing by 2.4-fold ($p < 0.05$) while AT2 and MAS levels remained unchanged compared to untreated cells (Malha et al., 2020; Gurwitz, 2020). Notably, the presence of HSA in both the experimental conditions tested resulted in a reversal of the RAS pathways balance compared to what was observed in Vero E6 cells infected with SARS-CoV-2 in the absence of HSA. Indeed, under both the experimental conditions tested, HSA caused a significant reduction in AT1 levels (4.4-fold, $p < 0.01$ in cells pre-treated with HSA and then infected; 2.2-fold, $p < 0.05$ in cells treated with the HSA:SARS-CoV2 mix) compared to SARS-CoV-2-infected cells. In contrast, a significant increase in the levels of ACE2 (2.7-fold, $p < 0.05$, in cells pre-treated with HSA and then infected; 1.9-fold, $p < 0.05$ in cells treated with the HSA:SARS-CoV2 mix), AT2 (3.4-fold, $p < 0.05$ in cells pre-treated with HSA and then infected; 7-fold, $p < 0.05$ in cells treated with the HSA:SARS-CoV2 mix), and MAS (2.3-fold, $p < 0.05$ in cells pre-treated with HSA and then infected; 6.8-fold, $p < 0.05$ in cells treated with the HSA:SARS-CoV2 mix) was observed compared to SARS-COV-2-treated cells (Fig. 4).

Overall, these data clearly support the protective role of HSA towards SARS-CoV-2 infection. Indeed, HSA results able to inhibit the virus proliferation and to induce the protective arm of the protective ACE2/Ang 1–7/MAS/AT2 axis of RAS.

3.5. The levels of HSA decrease in PBMCs derived from COVID-19 hypoalbuminemic patients compared to COVID-19 normoalbuminemic patients

It has been reported that HSA internalizes in leukocytes of patients with acutely decompensated cirrhosis, potentially fulfilling its immunomodulatory functions (Casulleras et al., 2020; Saha et al., 2022). With the aim of investigating the hypothesis that hypoalbuminemia in COVID-19 patients could be attributed to the relocalization of albumin into PBMCs (Casulleras et al., 2020; Saha et al., 2022; Chu et al., 2020), we performed a preliminary pilot study that involved 16 hospitalized COVID-19 patients, of which 9 were normoalbuminemic (HSA levels ≥ 3.5 g/dL) and 7 hypoalbuminemic (HSA levels < 3.5 g/dL) (Fig. 5A). Peripheral blood samples were collected from these patients, and HSA levels were determined in PBMCs using immunoblotting. For each patient, both intracellular PBMCs and plasma HSA levels were assessed. The results obtained indicated a reduction in HSA levels in the PBMCs of hypoalbuminemic patients compared to normoalbuminemic ones (Fig. 5B). This finding suggests that hypoalbuminemia in COVID-19 patients is not primarily caused by the relocalization of albumin, but rather by an overall decrease in HSA levels.

4. Discussion

Hypoalbuminemia has been reported in COVID-19 patients and is considered an indicator of the disease severity and prognosis (Huang et al., 2020; Sanson et al., 2023; Zerbato et al., 2022; Chen et al., 2021; Violi et al., 2020). The underlying mechanisms by which low HSA levels correlate with poor outcomes in COVID-19 are not fully understood, but it is quite clear that hypoalbuminemia is associated with the acquisition and severity of infectious diseases, and that the severity of hypoalbuminemia reflects the seriousness of both acute and chronic inflammation (Vita et al., 2020; di Masi et al., 2018; Di Bella et al., 2015; Di Bella et al., 2016; Minatoguchi et al., 2018; Soeters et al., 2019; Johnson and Winlow, 2022; Wiedermann, 2022). In this study, our aim was to clarify the molecular basis of the correlation between HSA levels and susceptibility to SARS-CoV-2 infection.

Our results support the notion that HSA acts as a self-defense mechanism by binding to the S1 domain of the spike protein with a K_d value of $\sim 2.6 \times 10^{-6}$ M. Serum proteins, which are highly abundant in human plasma, are emerging as key players in the host-pathogen interactions, thus influencing the onset and the severity of infections (Wiedermann, 2022). Indeed, we previously reported that HSA acts as a buffer capable of binding and transporting various ligands (*e.g.*, metal ions, drugs, heme), as well as reducing the activity of bacterial and fungal toxins. Consequently, inadequate albumin buffering (*i.e.*, in patients with hypoalbuminemia) has been associated with a greater

A

Patient	Plasma HSA levels (g/L)	N/H
#1	3.66	N
#2	4.03	N
#3	4.01	N
#4	3.86	N
#5	3.85	N
#6	3.85	N
#7	3.81	N
#8	3.82	N
#9	4.13	N
#10	2.63	H
#11	2.69	H
#12	2.71	H
#13	2.64	H
#14	2.78	H
#15	2.79	H
#16	2.78	H

B

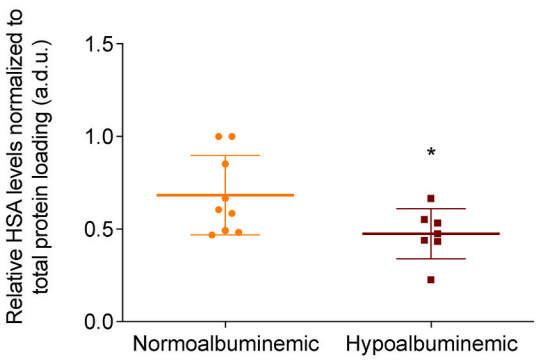

Fig. 5. The levels of HSA in PBMCs decrease in hypoalbuminemic patients infected by SARS-CoV-2. Plasma was collected from 9 normoalbuminemic and 7 hypolbuminemic COVID-19 patients and PBMCs were collected. (**A**) Plasma levels of HSA were determined and reported as g/L. (**B**) Intracellular levels of HSA were measured by immunoblot using an anti-HSA antibody and data were normalized to the total protein loading as visualized by Coomassie staining. The graph reports the medians ± SD of HSA levels (Student's t-test *p < 0.05, with respect to the normoalbuminemic patients).

susceptibility to pathogenic infections and systemic complications (Vita et al., 2020; di Masi et al., 2018; Di Bella et al., 2015; Di Bella et al., 2016; Austermeier et al., 2021; De Simone et al., 2023). Molecular docking results predicted that domains I and III of HSA interact with S1 though numerous bonds. The Lys517 and Lys524 residues, both located in domain III of HSA and critical for S1 recognition, can undergo glycation. Notably, it has been previously reported that the binding capacity of native albumin to the S1 subunit decreases with increasing concentration of glycated albumin (Zekri-Nechar et al., 2022; Iles et al., 2022). This supports our data, highlighting the key role played by the domain III of HSA in spike recognition. On the other side, the Arg466, Asn487, Tyr489, and Gln493 residues located in the RBM of the RDB region of S1 play are critical in the interaction with HSA. Intriguingly, the RBM region of S1, specifically the Lys417, Asn487, Tyr489, Gln493 residues, are also involved in ACE2 recognition (Lan et al., 2020). The HSA:S1 complex predicted here appears similar to one of the models obtained through molecular docking and all-atom molecular dynamics simulations reported by Yin and colleagues (Yin et al., 2021). Specifically, our results align with model 2 which indicates that the RBD of spike binds to the junction of domain I and domain III of HSA, with electrostatic energy and van der Waals forces playing crucial roles in the interaction. Notably, the binding energy of the HSA:RBD complex, calculated using the screening MM/PBSA method, was significantly stronger than that of ACE2:RBD, thereby confirming that HSA has the potential to effectively neutralize the RBD of Spike (Yin et al., 2021).

The molecular docking results here reported are further corroborated by displacement ELISA experiments confirming the competition of HSA and ACE2 for binding to S1. Although HSA binding affinity for S1 falls within the micromolar range, whereas ACE2 affinity for S1 is in the nanomolar range (Lu et al., 2020) (data reported here), the high plasma concentration of HSA in normoalbuminemic subjects (3.5–5.5 g/dL) increases the likelihood of interaction between HSA and SARS-CoV-2, thus compensating for the relatively low affinity between HSA and spike protein. This hypothesis finds an experimental support in the HSA protective effect reported in Vero E6 infected with SARS-CoV-2 delta variant AY61 sub-lineage. Indeed, HSA decreases the viral replication rate of SARS-CoV-2.

Besides, we reported that HSA exerts a protective effect against SARS-CoV-2 infection by inducing the protective arm of the RAS pathway (i.e., the ACE2/Ang 1–7/MAS/AT2 axis), at least when administered before infection. RAS operates via a tightly regulated mechanism involving enzymes and hormones expressed in various organs (Pahlavani et al., 2017; Nehme et al., 2019). The RAS system is finely regulated by ACE and ACE2 receptors, governing the equilibrium between classical and protective RAS pathways. However, this equilibrium is disrupted in SARS-CoV-2-infected patients, as ACE2 binding to the spike protein significantly reduces ACE2 enzymatic activity (Mascolo et al., 2020; Ashraf et al., 2021; Rysz et al., 2021; Gao et al., 2022; Oudit et al., 2023). Consequently, the RAS pathway becomes dramatically skewed in COVID-19 patients toward the classical axis, leading to increased levels of circulating Ang II and decreased Ang 1–7 (Gao et al., 2022; Oudit et al., 2023; Braga et al., 2020; Lissoni et al., 2020; Miesbach, 2020; Silhol et al., 2020; Dean et al., 2021; Osman et al., 2021). This shift in angiotensin levels disrupts RAS balance, possibly resulting in elevated harmful effects, including vasoconstriction, inflammation, and pro-fibrotic signaling (Ni et al., 2020; Rysz et al., 2021; Gao et al., 2022; Oudit et al., 2023). Interestingly, we found that HSA counteracts the classical pathway induced by SARS-CoV-2 infection by inducing ACE2, AT2, and MAS, which are components of the protective arm of the RAS pathway responsible for anti-thrombotic, anti-inflammatory, and vasodilatory effects (Fig. 6). This outcome aligns with earlier research suggesting that HSA modulates the expression and activity of ACE and ACE2, and influences the production of angiotensin(s) (Liu et al., 2009; Márquez et al., 2014).

HSA internalizes in leukocytes of patients with acutely decompensated cirrhosis to attend its immunomodulatory function(s) (Casulleras et al., 2020). Given this, we investigated whether HSA might shift from plasma to PBMC cells in response to SARS-CoV-2 infection, potentially contributing to the reported hypoalbuminemia. Our results reveal that in hypoalbuminemic COVID-19 patients, HSA levels in PBMCs were lower compared to normoalbuminemic COVID-19 patients. This suggests that hypoalbuminemia in COVID-19 patients is not due to albumin re-localization but rather to a global decrease in HSA levels, possibly linked to its movement into the extravascular space or interstitium, driven by inflammation-induced vascular leakage (Soeters et al., 2019).

Despite the numerous receptors able to bind to HSA (Vita et al., 2022; Ishima et al., 2022; Li et al., 2023), it is challenging to hypothesize that HSA mediates the internalization of SARS-CoV-2. Indeed, molecular dynamics analyses have demonstrated that although the RBD of spike occupies the region of HSA involved in the recognition of the neonatal Fc receptor (FcRn) (Chaudhury et al., 2003), it is possible to exclude a so-called "antibody-dependent enhancement (ADE)" effect (Yin et al., 2021). ADE represents the mechanism through which the binding of a virus to the host antibodies/proteins enhances its entry into host cells. Therefore, the available data led to exclude the hypothesis that

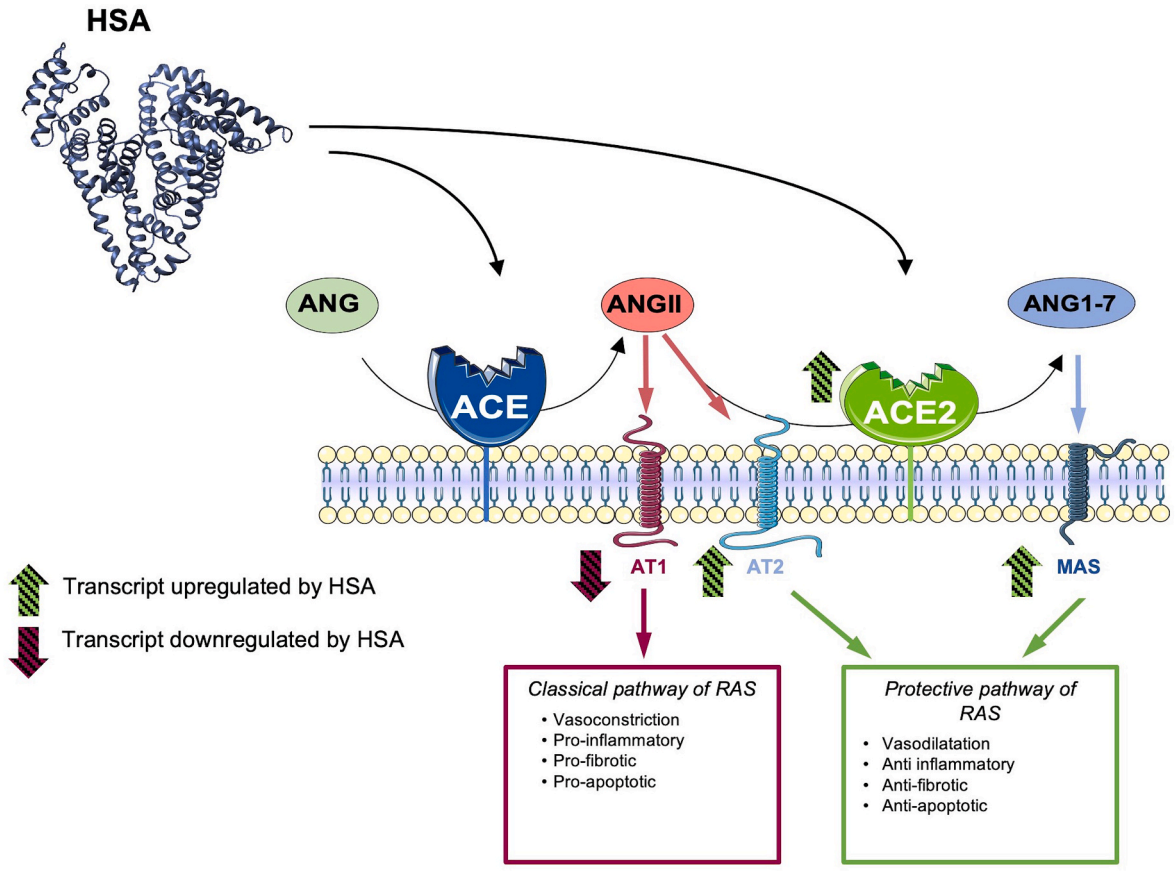

Fig. 6. Proposed model for explaining the protective role of HSA towards SARS-CoV-2 infection. A fine balance between the classic and protective pathways of the Renin-Angiotensin System (RAS), under physiological conditions, exists. During SARS-CoV-2 infection, ACE2 is downregulated, leading to an increase in Angiotensin II (Ang II) and Angiotensin 1-7 (Ang 1–7) levels, which promotes the ACE/Ang II/AT2 axis, subsequently triggering a pro-inflammatory and a pro-fibrotic response. In normoalbuminemic individuals, HSA upregulates ACE2, AT2, and MAS, promoting the ACE2/Ang 1–7/AT2-MAS axis. This, in turn, induces anti-inflammatory and anti-fibrotic responses. Therefore, HSA appears to counteract the effects of SARS-CoV-2 on the RAS pathway, contributing to the maintenance of a physiological RAS balance. As a consequence, in hypoalbuminemic patients with COVID-19, the low levels of HSA impede the modulation of the protective arm of RAS. Consequently, the ACE/AngII/AT2 axis triggers the reported pro-inflammatory and pro-fibrotic effects.

SARS-CoV-2 exploits the interaction with HSA to enter specific cells without relying on the ACE2 pathway. Indeed, if HSA could mediate the entry of SARS-CoV-2 into host cells, the virus would have posed a significant threat to the normoalbuminemic population. On the contrary, it has been reported that hypoalbuminemia predisposes individuals to the worst outcomes of the infection. This suggests that HSA does not facilitate viral entry but instead exerts a neutralizing effect against pathogens in plasma.

5. Conclusions

The data reported here support the notion that hypoalbuminemia exacerbates the imbalance of the RAS pathway towards the classical "harmful" axis. This could help explain the greater severity and increased mortality rates observed in hypoalbuminemic individuals with COVID-19. In addition to its role in regulating the RAS pathway, specifically by promoting the protective arm, HSA binds to the Spike protein and competes with ACE2. This suggests that reduced levels of circulating HSA in hypoalbuminemic patients may render them more susceptible to SARS-CoV-2 infection, as spike protein is free to bind to ACE2 and enter human cells. Interestingly, the effects of HSA on the RAS pathway resemble those of angiotensin receptor blockers (ARBs) and ACE inhibitors, which have been proposed as potential therapeutic strategies to mitigate acute inflammation and vasoconstriction during COVID-19 (Li et al., 2021; Shukla and Banerjee, 2021; Kuzeytemiz and Tenekecioglu, 2022).

The demonstration of HSA capability to bind the RBD of spike and to modulate RAS signaling could be relevant to support albumin use as an adjuvant in the treatment of COVID infections. Indeed, it is conceivable that treatment with albumin preparations or agents containing albumin may sustain the anti-viral therapy. Overall, an increased understanding of the non-oncotic functions of HSA, and particularly of its role in the innate immunity response, will help improve the risk/benefit assessment and selection of optimal therapeutic regimen for a wide array of infectious diseases and patient types. In this context, greater clinical attention to HSA concentration is warranted for older patients, for patients treated with multiple drugs that could potentially affect or be affected by HSA concentration, as well as for patients with multiple comorbidities.

For the future, additional *in vivo* studies will be necessary to substantiate the ability of HSA to neutralize spike function and reduce virus entry into host cells. In this context, particular attention should be given to SARS-CoV-2 variants in which the mutation is localized within the interface involved in HSA recognition. Indeed, beside the Delta variant (K417 N; PANGO lineage: B.1.617.2) here studied, which involves the Lys417 residue located in the interface of interaction between spike and HSA, further mutations of this amino acid have been reporter in the Beta (K417 N; PANGO lineage: B.1.351) and Gamma (K417T; PANGO lineage: P.1) variants (Jackson et al., 2022). Additionally, also the Gln493 residue results mutated in the Omicron variant (Q493R; PANGO lineage: B.1.1.529) (da Costa et al., 2022; Antony et al., 2022). Therefore, it will be of interest to study the effects of these natural mutations of the spike

RBD on HSA recognition and neutralization activities.

Declaration of competing interest

The authors declare that they have no known competing financial interests or personal relationships that could have appeared to influence the work reported in this paper.

Acknowledgments

A.d.M gratefully acknowledges the Grant of Dipartimento di Eccellenza 2018–2022 and 2023–2027 from MIUR (Legge 232/2016, Articolo 1, Comma 314–337). R.V. is a PhD student at the Department of Sciences of the Roma Tre University (Rome, Italy). G.M.V. worked at this paper during the period in which he was PhD student at the Department of Sciences of the Roma Tre University (Rome, Italy). We thank Prof. Fabio Polticelli, Bruna Marini and Rudy Ippodrino for helpful discussion.

Appendix A. Supplementary data

Supplementary data to this article can be found online at https://doi.org/10.1016/j.amolm.2023.100033.

References

Almehdi, A.M., Khoder, G., Alchakee, A.S., Alsayyid, A.T., Sarg, N.H., Soliman, S.S.M., 2021. SARS-CoV-2 spike protein: pathogenesis, vaccines, and potential therapies. Infection 49, 855–876. https://doi.org/10.1007/s15010-021-01677-8.

Antony, P., Jobe, A., Vijayan, R., 2022. Dynamics of the interaction between the receptor-binding domain of SARS-CoV-2 Omicron (B.1.1.529) variant and human angiotensin-converting enzyme 2. PeerJ 10, e13680. https://doi.org/10.7717/peerj.13680.

Araujo, D.B., Machado, R.R.G., Amgarten, D.E., Malta, F. de M., de Araujo, G.G., Monteiro, C.O., Candido, E.D., Soares, C.P., de Menezes, F.G., Pires, A.C.C., Santana, R.A.F., Viana, A. de O., Dorlass, E., Thomazelli, L., Ferreira, L.C. de S., Botosso, V.F., Carvalho, C.R.G., Oliveira, D.B.L., Pinho, J.R.R., Durigon, E.L., 2020. SARS-CoV-2 isolation from the first reported patients in Brazil and establishment of a coordinated task network. Mem. Inst. Oswaldo Cruz 115. https://doi.org/10.1590/0074-02760200342.

Ashraf, U.M., Abokor, A.A., Edwards, J.M., Waigi, E.W., Royfman, R.S., Hasan, S.A.-M., Smedlund, K.B., Hardy, A.M.G., Chakravarti, R., Koch, L.G., 2021. SARS-CoV-2, ACE2 expression, and systemic organ invasion. Physiol. Genom. 53, 51–60. https://doi.org/10.1152/physiolgenomics.00087.2020.

Austermeier, S., Pekmezović, M., Porschitz, P., Lee, S., Kichik, N., Moyes, D.L., Ho, J., Kotowicz, N.K., Naglik, J.R., Hube, B., Gresnigt, M.S., 2021. Albumin neutralizes hydrophobic toxins and modulates candida albicans pathogenicity. mBio 12. https://doi.org/10.1128/mBio.00531-21.

Bakker, J., Horowitz, J.M., Hagedorn, J., Kozloff, S., Kaufman, D., Castro, R., 2021. Blood volume and albumin transudation in critically ill COVID-19 patients. Crit. Care 25, 269. https://doi.org/10.1186/s13054-021-03699-y.

Banu, N., Panikar, S.S., Leal, L.R., Leal, A.R., 2020. Protective role of ACE2 and its downregulation in SARS-CoV-2 infection leading to Macrophage Activation Syndrome: therapeutic implications. Life Sci. 256, 117905 https://doi.org/10.1016/j.lfs.2020.117905.

Bayarri-Olmos, R., Rosbjerg, A., Johnsen, L.B., Helgstrand, C., Bak-Thomsen, T., Garred, P., Skjoedt, M.-O., 2021. The SARS-CoV-2 Y453F mink variant displays a pronounced increase in ACE-2 affinity but does not challenge antibody neutralization. J. Biol. Chem. 296, 100536 https://doi.org/10.1016/j.jbc.2021.100536.

Bian, J., Li, Z., 2021. Angiotensin-converting enzyme 2 (ACE2): SARS-CoV-2 receptor and RAS modulator. Acta Pharm. Sin. B 11, 1–12. https://doi.org/10.1016/j.apsb.2020.10.006.

Bielarz, V., Willemart, K., Avalosse, N., De Swert, K., Lotfi, R., Lejeune, N., Poulain, F., Ninanne, N., Gilloteaux, J., Gillet, N., Nicaise, C., 2021. Susceptibility of neuroblastoma and glioblastoma cell lines to SARS-CoV-2 infection. Brain Res. 1758, 147344 https://doi.org/10.1016/j.brainres.2021.147344.

Bosso, H., Soares Arantes, G.E.P., Barbalho, S.M., Guiguer, É.L., de Souza, M. da S.S., Bueno, P.C. dos S., Chies, A.B., de Oliveira, P.B., Mendes, C.G., Araújo, A.C., 2019. Effects of green and ripe coffee in the metabolic profile and muscle enzymes in animals practicing physical exercise. J. Med. Food 22, 416–420. https://doi.org/10.1089/jmf.2018.0162.

Böyum, A, 1968. Isolation and removal of lymphocytes from bone marrow of rats and guinea-pigs. Scand J. Clin. Lab. Invest. Suppl. 97, 91–106. PMID: 4179069.

Braga, C.L., Silva-Aguiar, R.P., Battaglini, D., Peruchetti, D.B., Robba, C., Pelosi, P., Rocco, P.R.M., Caruso-Neves, C., Silva, P.L., 2020. The renin–angiotensin–aldosterone system: role in pathogenesis and potential therapeutic target in COVID-19. Pharmacol Res Perspect 8. https://doi.org/10.1002/prp2.623.

Cardillo, L., de Martinis, C., Viscardi, M., Esposito, C., Sannino, E., Lucibelli, G., Limone, A., Pellino, S., Anastasio, R., Pellicanò, R., Baldi, L., Galiero, G., Fusco, G., 2021. SARS-CoV-2 quantitative real time PCR and viral loads analysis among asymptomatic and symptomatic patients: an observational study on an outbreak in two nursing facilities in Campania Region (Southern Italy). Infect. Agents Cancer 16, 45. https://doi.org/10.1186/s13027-021-00388-x.

Carrasco-Sánchez, F.J., López-Carmona, M.D., Martínez-Marcos, F.J., Pérez-Belmonte, L. M., Hidalgo-Jiménez, A., Buonaiuto, V., Suárez Fernández, C., Freire Castro, S.J., Luordo, D., Pesqueira Fontan, P.M., Blázquez Encinar, J.C., Magallanes Gamboa, J. O., de la Peña Fernández, A., Torres Peña, J.D., Fernández Solà, J., Napal Lecumberri, J.J., Amorós Martínez, F., Guisado Espartero, M.E., Jorge Ripper, C., Gómez Méndez, R., Vicente López, N., Román Bernal, B., Rojano Rivero, M.G., Ramos Rincón, J.M., Gómez Huelgas, R., 2021. Admission hyperglycaemia as a predictor of mortality in patients hospitalized with COVID-19 regardless of diabetes status: data from the Spanish SEMI-COVID-19 Registry. Ann. Med. 53, 103–116. https://doi.org/10.1080/07853890.2020.1836566.

Casulleras, M., Flores-Costa, R., Duran-Güell, M., Alcaraz-Quiles, J., Sanz, S., Titos, E., López-Vicario, C., Fernández, J., Horrillo, R., Costa, M., de la Grange, P., Moreau, R., Arroyo, V., Clària, J., 2020. Albumin internalizes and inhibits endosomal TLR signaling in leukocytes from patients with decompensated cirrhosis. Sci. Transl. Med. 12 https://doi.org/10.1126/scitranslmed.aax5135.

Chaudhury, C., Mehnaz, S., Robinson, J.M., Hayton, W.L., Pearl, D.K., Roopenian, D.C., Anderson, C.L., 2003. The major histocompatibility complex-related Fc receptor for IgG (FcRn) binds albumin and prolongs its lifespan. J. Exp. Med. 197, 315–322. https://doi.org/10.1084/jem.20021829.

Chen, C., Zhang, Y., Zhao, X., Tao, M., Yan, W., Fu, Y., 2021. Hypoalbuminemia – an indicator of the severity and prognosis of COVID-19 patients: a multicentre retrospective analysis. Infect. Drug Resist. 14, 3699–3710. https://doi.org/10.2147/IDR.S327090.

Chu, X., Karasinski, K., Donellan, S., Kaniper, S., Wood, G.C., Shi, W., Edwards, M.A., Soans, R., Still, C.D., Gerhard, G.S., 2020. A retrospective case control study identifies peripheral blood mononuclear cell albumin RNA expression as a biomarker for non-alcoholic fatty liver disease. Langenbeck's Arch. Surg. 405, 165–172. https://doi.org/10.1007/s00423-019-01848-0.

da Costa, C.H.S., de Freitas, C.A.B., Alves, C.N., Lameira, J., 2022. Assessment of mutations on RBD in the spike protein of SARS-CoV-2 alpha, delta and Omicron variants. Sci. Rep. 12, 8540. https://doi.org/10.1038/s41598-022-12479-9.

da Silva Torres, M.K., Bichara, C.D.A., de Almeida, M. de N. do S., Vallinoto, M.C., Queiroz, M.A.F., Vallinoto, I.M.V.C., dos Santos, E.J.M., de Carvalho, C.A.M., Vallinoto, A.C.R., 2022. The complexity of SARS-CoV-2 infection and the COVID-19 pandemic. Front. Microbiol. 13 https://doi.org/10.3389/fmicb.2022.789882.

De Simone, G., Varricchio, R., Ruberto, T.F., di Masi, A., Ascenzi, P., 2023. Heme scavenging and delivery: the role of human serum albumin. Biomolecules 13, 575. https://doi.org/10.3390/biom13030575.

de Vries, S.J., Bonvin, A.M.J.J., 2011. CPORT: a consensus interface predictor and its performance in prediction-driven docking with HADDOCK. PLoS One 6, e17695. https://doi.org/10.1371/journal.pone.0017695.

Dean, A.Q., Bozza, W.P., Twomey, J.D., Luo, S., Nalli, A., Zhang, B., 2021. The fight against COVID-19: striking a balance in the renin–angiotensin system. Drug Discov. Today 26, 2214–2220. https://doi.org/10.1016/j.drudis.2021.04.006.

Di Bella, S., di Masi, A., Turla, S., Ascenzi, P., Gouliouris, T., Petrosillo, N., 2015. The protective role of albumin in *Clostridium difficile* infection: a step toward solving the puzzle. Infect. Control Hosp. Epidemiol. 36, 1478–1480. https://doi.org/10.1017/ice.2015.221.

Di Bella, S., Ascenzi, P., Siarakas, S., Petrosillo, N., di Masi, A., 2016. Clostridium difficile toxins A and B: insights into pathogenic properties and extraintestinal effects. Toxins 8, 134. https://doi.org/10.3390/toxins8050134.

di Masi, A., Leboffe, L., Polticelli, F., Tonon, F., Zennaro, C., Caterino, M., Stano, P., Fischer, S., Hägele, M., Müller, M., Kleger, A., Papatheodorou, P., Nocca, G., Arcovito, A., Gori, A., Ruoppolo, M., Barth, H., Petrosillo, N., Ascenzi, P., Di Bella, S., 2018. Human serum albumin is an essential component of the host defense mechanism against Clostridium difficile intoxication. J. Infect. Dis. 218, 1424–1435. https://doi.org/10.1093/infdis/jiy338.

Fanali, G., di Masi, A., Trezza, V., Marino, M., Fasano, M., Ascenzi, P., 2012. Human serum albumin: from bench to bedside. Mol. Aspect. Med. 33, 209–290. https://doi.org/10.1016/j.mam.2011.12.002.

Forrester, S.J., Booz, G.W., Sigmund, C.D., Coffman, T.M., Kawai, T., Rizzo, V., Scalia, R., Eguchi, S., 2018. Angiotensin II signal transduction: an update on mechanisms of physiology and pathophysiology. Physiol. Rev. 98, 1627–1738. https://doi.org/10.1152/physrev.00038.2017.

Gao, X., Zhang, S., Gou, J., Wen, Y., Fan, L., Zhou, J., Zhou, G., Xu, G., Zhang, Z., 2022. Spike-mediated ACE2 down-regulation was involved in the pathogenesis of SARS-CoV-2 infection. J. Infect. 85, 418–427. https://doi.org/10.1016/j.jinf.2022.06.030.

Georgieva, E., Atanasov, V., Kostandieva, R., Tsoneva, V., Mitev, M., Arabadzhiev, G., Yovchev, Y., Karamalakova, Y., Nikolova, G., 2023. Direct application of 3-maleimido-PROXYL for proving hypoalbuminemia in cases of SARS-CoV-2 infection: the potential diagnostic method of determining albumin instability and oxidized protein level in severe COVID-19. Int. J. Mol. Sci. 24, 5807. https://doi.org/10.3390/ijms24065807.

Gioia, M., Ciaccio, C., Calligari, P., De Simone, G., Sbardella, D., Tundo, G., Fasciglione, G.F., Di Masi, A., Di Pierro, D., Bocedi, A., Ascenzi, P., Coletta, M., 2020. Role of proteolytic enzymes in the COVID-19 infection and promising therapeutic approaches. Biochem. Pharmacol. 182, 114225 https://doi.org/10.1016/j.bcp.2020.114225.

Gurwitz, D., 2020. Angiotensin receptor blockers as tentative SARS-CoV-2 therapeutics. Drug Dev. Res. 81, 537–540. https://doi.org/10.1002/ddr.21656.

Hoffmann, M., Kleine-Weber, H., Schroeder, S., Krüger, N., Herrler, T., Erichsen, S., Schiergens, T.S., Herrler, G., Wu, N.-H., Nitsche, A., Müller, M.A., Drosten, C., Pöhlmann, S., 2020. SARS-CoV-2 cell entry depends on ACE2 and TMPRSS2 and is blocked by a clinically proven protease inhibitor. Cell 181, 271–280.e8. https://doi.org/10.1016/j.cell.2020.02.052.

Honorato, R.V., Koukos, P.I., Jiménez-García, B., Tsaregorodtsev, A., Verlato, M., Giachetti, A., Rosato, A., Bonvin, A.M.J.J., 2021. Structural biology in the clouds: the WeNMR-EOSC ecosystem. Front. Mol. Biosci. 8 https://doi.org/10.3389/fmolb.2021.729513.

Huang, J., Cheng, A., Kumar, R., Fang, Y., Chen, G., Zhu, Y., Lin, S., 2020. Hypoalbuminemia predicts the outcome of COVID-19 independent of age and co-morbidity. J. Med. Virol. 92, 2152–2158. https://doi.org/10.1002/jmv.26003.

Huang, Y., Harris, B.S., Minami, S.A., Jung, S., Shah, P.S., Nandi, S., McDonald, K.A., Faller, R., 2022. SARS-CoV-2 spike binding to ACE2 is stronger and longer ranged due to glycan interaction. Biophys. J. 121, 79–90. https://doi.org/10.1016/j.bpj.2021.12.002.

Iles, J., Zmuidinaite, R., Sadee, C., Gardiner, A., Lacey, J., Harding, S., Ule, J., Roblett, D., Heeney, J., Baxendale, H., Iles, R.K., 2022. SARS-CoV-2 spike protein binding of glycated serum albumin—its potential role in the pathogenesis of the COVID-19 clinical syndromes and bias towards individuals with pre-diabetes/type 2 diabetes and metabolic diseases. Int. J. Mol. Sci. 23, 4126. https://doi.org/10.3390/ijms23084126.

Ishima, Y., Maruyama, T., Otagiri, M., Chuang, V.T.G., Ishida, T., 2022. The New delivery strategy of albumin carrier utilizing the interaction with albumin receptors. Chem. Pharm. Bull. (Tokyo) 70, 330–333. https://doi.org/10.1248/cpb.c21-01024.

Jackson, C.B., Farzan, M., Chen, B., Choe, H., 2022. Mechanisms of SARS-CoV-2 entry into cells. Nat. Rev. Mol. Cell Biol. 23, 3–20. https://doi.org/10.1038/s41580-021-00418-x.

Johnson, A.S., Winlow, W., 2022. COVID-19 vulnerabilities are intensified by declining human serum albumin levels. Exp. Physiol. 107, 674–682. https://doi.org/10.1113/EP089703.

Kheir, M., Saleem, F., Wang, C., Mann, A., Chua, J., 2021. Higher albumin levels on admission predict better prognosis in patients with confirmed COVID-19. PLoS One 16, e0248358. https://doi.org/10.1371/journal.pone.0248358.

Kirtipal, N., Kumar, S., Dubey, S.K., Dwivedi, V.D., Gireesh Babu, K., Malý, P., Bharadwaj, S., 2022. Understanding on the possible routes for SARS CoV-2 invasion via ACE2 in the host linked with multiple organs damage. Infect. Genet. Evol. 99, 105254 https://doi.org/10.1016/j.meegid.2022.105254.

Kuzeytemiz, M., Tenekecioglu, E., 2022. Effect of renin-angiotensin system blocker on COVID-19 in young patients with hypertension. J. Invest. Med. 70, 786–791. https://doi.org/10.1136/jim-2021-002036.

Lan, J., Ge, J., Yu, J., Shan, S., Zhou, H., Fan, S., Zhang, Q., Shi, X., Wang, Q., Zhang, L., Wang, X., 2020. Structure of the SARS-CoV-2 spike receptor-binding domain bound to the ACE2 receptor. Nature 581, 215–220. https://doi.org/10.1038/s41586-020-2180-5.

Li, M., Wang, Y., Ndiwane, N., Orner, M.B., Palacios, N., Mittler, B., Berlowitz, D., Kazis, L.E., Xia, W., 2021. The association of COVID-19 occurrence and severity with the use of angiotensin converting enzyme inhibitors or angiotensin-II receptor blockers in patients with hypertension. PLoS One 16, e0248652. https://doi.org/10.1371/journal.pone.0248652.

Li, X.-L., Yan, Z.-S., Ma, Y.-Q., Ding, H.-M., 2023. Effect of maleylation and denaturation of human serum albumin on its interaction with scavenger receptors. Proteins 91, 1140–1151. https://doi.org/10.1002/prot.26499.

Lissoni, P., Rovelli, F., Monzon, A., Messina, G., Porta, E., Porro, G., Pensato, S., Martin, E., Sassola, A., Caddeo, A., Galli, C., Merli, N., Valentini, A., Di Fede, G., 2020. COVID-19 Disease as an Acute Angiotensin 1-7 Deficiency: A Preliminary Phase 2 Study with Angiotensin 1-7 in Association with Melatonin and Cannabidiol in Symptomatic COVID19 -Infected Subjects.

Liu, B.-C., Gao, J., Li, Q., Xu, L.-M., 2009. Albumin caused the increasing production of angiotensin II due to the dysregulation of ACE/ACE2 expression in HK2 cells. Clin. Chim. Acta 403, 23–30. https://doi.org/10.1016/j.cca.2008.12.015.

Lu, R., Zhao, X., Li, J., Niu, P., Yang, B., Wu, H., Wang, W., Song, H., Huang, B., Zhu, N., Bi, Y., Ma, X., Zhan, F., Wang, L., Hu, T., Zhou, H., Hu, Z., Zhou, W., Zhao, L., Chen, J., Meng, Y., Wang, J., Lin, Y., Yuan, J., Xie, Z., Ma, J., Liu, W.J., Wang, D., Xu, W., Holmes, E.C., Gao, G.F., Wu, G., Chen, W., Shi, W., Tan, W., 2020. Genomic characterisation and epidemiology of 2019 novel coronavirus: implications for virus origins and receptor binding. Lancet 395, 565–574. https://doi.org/10.1016/S0140-6736(20)30251-8.

Malha, L., Mueller, F.B., Pecker, M.S., Mann, S.J., August, P., Feig, P.U., 2020. COVID-19 and the renin-angiotensin system. Kidney Int Rep 5, 563–565. https://doi.org/10.1016/j.ekir.2020.03.024.

Márquez, E., Riera, M., Pascual, J., Soler, M.J., 2014. Albumin inhibits the insulin-mediated ACE2 increase in cultured podocytes. Am. J. Physiol. Ren. Physiol. 306, F1327–F1334. https://doi.org/10.1152/ajprenal.00594.2013.

Mascolo, A., Scavone, C., Rafaniello, C., Ferrajolo, C., Racagni, G., Berrino, L., Paolisso, G., Rossi, F., Capuano, A., 2020. Renin-angiotensin system and coronavirus disease 2019: a narrative review. Front Cardiovasc Med 7. https://doi.org/10.3389/fcvm.2020.00143.

Miesbach, W., 2020. Pathological role of angiotensin II in severe COVID-19. TH Open 4, e138–e144. https://doi.org/10.1055/s-0040-1713678.

Minatoguchi, S., Nomura, A., Imaizumi, T., Sasaki, S., Ozeki, T., Uchida, D., Kawarazaki, H., Sasai, F., Tomita, K., Shimizu, H., Fujita, Y., 2018. Low serum albumin as a risk factor for infection-related in-hospital death among hemodialysis patients hospitalized on suspicion of infectious disease: a Japanese multicenter retrospective cohort study. Ren Replace Ther 4, 30. https://doi.org/10.1186/s41100-018-0173-8.

Nehme, A., Zouein, F.A., Zayeri, Z.D., Zibara, K., 2019. An update on the tissue renin angiotensin system and its role in physiology and pathology. J Cardiovasc Dev Dis 6, 14. https://doi.org/10.3390/jcdd6020014.

Ni, L., Ye, F., Cheng, M.-L., Feng, Y., Deng, Y.-Q., Zhao, H., Wei, P., Ge, J., Gou, M., Li, X., Sun, L., Cao, T., Wang, P., Zhou, C., Zhang, R., Liang, P., Guo, H., Wang, X., Qin, C.-F., Chen, F., Dong, C., 2020. Detection of SARS-CoV-2-specific humoral and cellular immunity in COVID-19 convalescent individuals. Immunity 52, 971–977.e3. https://doi.org/10.1016/j.immuni.2020.04.023.

Ogando, N.S., Dalebout, T.J., Zevenhoven-Dobbe, J.C., Limpens, R.W.A.L., van der Meer, Y., Caly, L., Druce, J., de Vries, J.J.C., Kikkert, M., Bárcena, M., Sidorov, I., Snijder, E.J., 2020. SARS-coronavirus-2 replication in Vero E6 cells: replication kinetics, rapid adaptation and cytopathology. J. Gen. Virol. 101, 925–940. https://doi.org/10.1099/jgv.0.001453.

Osman, I.O., Melenotte, C., Brouqui, P., Million, M., Lagier, J.-C., Parola, P., Stein, A., La Scola, B., Meddeb, L., Mege, J.-L., Raoult, D., Devaux, C.A., 2021. Expression of ACE2, soluble ACE2, angiotensin I, angiotensin II and angiotensin-(1-7) is modulated in COVID-19 patients. Front. Immunol. 12 https://doi.org/10.3389/fimmu.2021.625732.

Ou, X., Liu, Y., Lei, X., Li, P., Mi, D., Ren, L., Guo, L., Guo, R., Chen, T., Hu, J., Xiang, Z., Mu, Z., Chen, X., Chen, J., Hu, K., Jin, Q., Wang, J., Qian, Z., 2020. Characterization of spike glycoprotein of SARS-CoV-2 on virus entry and its immune cross-reactivity with SARS-CoV. Nat. Commun. 11, 1620. https://doi.org/10.1038/s41467-020-15562-9.

Oudit, G.Y., Wang, K., Viveiros, A., Kellner, M.J., Penninger, J.M., 2023. Angiotensin-converting enzyme 2—at the heart of the COVID-19 pandemic. Cell 186, 906–922. https://doi.org/10.1016/j.cell.2023.01.039.

Pahlavani, M., Kalupahana, NishanS., Ramalingam, L., Moustaid-Moussa, N., 2017. Regulation and functions of the renin-angiotensin system in white and Brown adipose tissue. In: Compr Physiol. Wiley, pp. 1137–1150. https://doi.org/10.1002/cphy.c160031.

Patel, S., Rauf, A., Khan, H., Abu-Izneid, T., 2017. Renin-angiotensin-aldosterone (RAAS): the ubiquitous system for homeostasis and pathologies. Biomed. Pharmacother. 94, 317–325. https://doi.org/10.1016/j.biopha.2017.07.091.

Paz Ocaranza, M., Riquelme, J.A., García, L., Jalil, J.E., Chiong, M., Santos, R.A.S., Lavandero, S., 2020. Counter-regulatory renin–angiotensin system in cardiovascular disease. Nat. Rev. Cardiol. 17, 116–129. https://doi.org/10.1038/s41569-019-0244-8.

Pettersen, E.F., Goddard, T.D., Huang, C.C., Couch, G.S., Greenblatt, D.M., Meng, E.C., Ferrin, T.E., 2004. UCSF Chimera?A visualization system for exploratory research and analysis. J. Comput. Chem. 25, 1605–1612. https://doi.org/10.1002/jcc.20084.

Rysz, S., Al-Saadi, J., Sjöström, A., Farm, M., Campoccia Jalde, F., Plattén, M., Eriksson, H., Klein, M., Vargas-Paris, R., Nyrén, S., Abdula, G., Ouellette, R., Granberg, T., Jonsson Fagerlund, M., Lundberg, J., 2021. COVID-19 pathophysiology may be driven by an imbalance in the renin-angiotensin-aldosterone system. Nat. Commun. 12, 2417. https://doi.org/10.1038/s41467-021-22713-z.

Saha, P., Moitra, P., Bhattacharjee, U., Bhattacharya, S., 2022. Selective pathological and intracellular detection of human serum albumin by photophysical and electrochemical techniques using a FRET-based molecular probe. Biosens. Bioelectron. 203, 114007 https://doi.org/10.1016/j.bios.2022.114007.

Salamanna, F., Maglio, M., Landini, M.P., Fini, M., 2020. Body localization of ACE-2: on the trail of the keyhole of SARS-CoV-2. Front. Med. 7 https://doi.org/10.3389/fmed.2020.594495.

Sambataro, G., Giuffrè, M., Sambataro, D., Palermo, A., Vignigni, G., Cesareo, R., Crimi, N., Torrisi, S.E., Vancheri, C., Malatino, L., Colaci, M., Del Papa, N., Pignataro, F., Roman-Pognuz, E., Fabbiani, M., Montagnani, F., Cassol, C., Cavagna, L., Zuccaro, V., Zerbato, V., Maurel, C., Luzzati, R., Di Bella, S., 2020. The model for early COvid-19 recognition (mecor) score: a proof-of-concept for a simple and low-cost tool to recognize a possible viral etiology in community-acquired pneumonia patients during COVID-19 outbreak. Diagnostics 10, 619. https://doi.org/10.3390/diagnostics10090619.

Sanson, G., De Nicolò, A., Zerbato, V., Segat, L., Koncan, R., Di Bella, S., Cusato, J., di Masi, A., Palermo, A., Caironi, P., D'Agaro, P., Luzzati, R., D'Avolio, A., 2023. A combined role for low vitamin D and low albumin circulating levels as strong predictors of worse outcome in COVID-19 patients. Ir. J. Med. Sci. 192, 423–430. https://doi.org/10.1007/s11845-022-02952-9.

Shukla, A.K., Banerjee, M., 2021. Angiotensin-converting-enzyme 2 and renin-angiotensin system inhibitors in COVID-19: an update. High Blood Pres. Cardiovasc. Prev. 28, 129–139. https://doi.org/10.1007/s40292-021-00439-9.

Silhol, F., Sarlon, G., Deharo, J.-C., Vaïsse, B., 2020. Downregulation of ACE2 induces overstimulation of the renin–angiotensin system in COVID-19: should we block the renin–angiotensin system? Hypertens. Res. 43, 854–856. https://doi.org/10.1038/s41440-020-0476-3.

Soetedjo, N.N.M., Iryaningrum, M.R., Damara, F.A., Permadhi, I., Sutanto, L.B., Hartono, H., Rasyid, H., 2021. Prognostic properties of hypoalbuminemia in COVID-19 patients: a systematic review and diagnostic meta-analysis. Clin Nutr ESPEN 45, 120–126. https://doi.org/10.1016/j.clnesp.2021.07.003.

Soeters, P.B., Wolfe, R.R., Shenkin, A., 2019. Hypoalbuminemia: pathogenesis and clinical significance. J. Parenter. Enteral Nutr. 43, 181–193. https://doi.org/10.1002/jpen.1451.

Sugio, S., Kashima, A., Mochizuki, S., Noda, M., Kobayashi, K., 1999. Crystal structure of human serum albumin at 2.5 Å resolution, Protein Engineering. Design and Selection 12, 439–446. https://doi.org/10.1093/protein/12.6.439.

Sun, D., Sang, Z., Kim, Y.J., Xiang, Y., Cohen, T., Belford, A.K., Huet, A., Conway, J.F., Sun, J., Taylor, D.J., Schneidman-Duhovny, D., Zhang, C., Huang, W., Shi, Y., 2021. Potent neutralizing nanobodies resist convergent circulating variants of SARS-CoV-2

by targeting diverse and conserved epitopes. Nat. Commun. 12, 4676. https://doi.org/10.1038/s41467-021-24963-3.
V Raghuvamsi, P., Tulsian, N.K., Samsudin, F., Qian, X., Purushotorman, K., Yue, G., Kozma, M.M., Hwa, W.Y., Lescar, J., Bond, P.J., MacAry, P.A., Anand, G.S., 2021. SARS-CoV-2 S protein:ACE2 interaction reveals novel allosteric targets. Elife 10. https://doi.org/10.7554/eLife.63646.
van Zundert, G.C.P., Rodrigues, J.P.G.L.M., Trellet, M., Schmitz, C., Kastritis, P.L., Karaca, E., Melquiond, A.S.J., van Dijk, M., de Vries, S.J., Bonvin, A.M.J.J., 2016. The HADDOCK2.2 web server: user-friendly integrative modeling of biomolecular complexes. J. Mol. Biol. 428, 720–725. https://doi.org/10.1016/j.jmb.2015.09.014.
Vangone, A., Bonvin, A., 2017. PRODIGY: a contact-based predictor of binding affinity in protein-protein complexes. Bio Protoc 7. https://doi.org/10.21769/BioProtoc.2124.
Violi, F., Ceccarelli, G., Cangemi, R., Alessandri, F., D'Ettorre, G., Oliva, A., Pastori, D., Loffredo, L., Pignatelli, P., Ruberto, F., Venditti, M., Pugliese, F., Mastroianni, C.M., 2020. Hypoalbuminemia, coagulopathy, and vascular disease in COVID-19. Circ. Res. 127, 400–401. https://doi.org/10.1161/CIRCRESAHA.120.317173.
Vita, G.M., De Simone, G., Leboffe, L., Montagnani, F., Mariotti, D., Di Bella, S., Luzzati, R., Gori, A., Ascenzi, P., di Masi, A., 2020. Human serum albumin binds streptolysin O (SLO) toxin produced by group A Streptococcus and inhibits its cytotoxic and hemolytic effects. Front. Immunol. 11 https://doi.org/10.3389/fimmu.2020.507092.
Vita, G.M., De Simone, G., De Marinis, E., Nervi, C., Ascenzi, P., di Masi, A., 2022. Serum albumin and nucleic acids biodistribution: from molecular aspects to biotechnological applications. IUBMB Life 74, 866–879. https://doi.org/10.1002/iub.2653.
Walls, A.C., Park, Y.-J., Tortorici, M.A., Wall, A., McGuire, A.T., Veesler, D., 2020. Structure, function, and antigenicity of the SARS-CoV-2 spike glycoprotein. Cell 181, 281–292.e6. https://doi.org/10.1016/j.cell.2020.02.058.
Wan, Y., Shang, J., Graham, R., Baric, R.S., Li, F., 2020. Receptor recognition by the novel coronavirus from wuhan: an analysis based on decade-long structural studies of SARS coronavirus. J. Virol. 94 https://doi.org/10.1128/JVI.00127-20.
Wiedermann, C.J., 2022. Use of hyperoncotic human albumin solution in severe traumatic brain injury revisited—a narrative review and meta-analysis. J. Clin. Med. 11, 2662. https://doi.org/10.3390/jcm11092662.
Wrapp, D., Wang, N., Corbett, K.S., Goldsmith, J.A., Hsieh, C.-L., Abiona, O., Graham, B. S., McLellan, J.S., 2020. Cryo-EM structure of the 2019-nCoV spike in the prefusion conformation. Science (1979) 367, 1260–1263. https://doi.org/10.1126/science.abb2507.
Wu, M.A., Fossali, T., Pandolfi, L., Carsana, L., Ottolina, D., Frangipane, V., Rech, R., Tosoni, A., Lopez, G., Agarossi, A., Cogliati, C., Meloni, F., Marchini, B., Nebuloni, M., Catena, E., Colombo, R., 2021. Hypoalbuminemia in COVID-19: assessing the hypothesis for underlying pulmonary capillary leakage. J. Intern. Med. 289, 861–872. https://doi.org/10.1111/joim.13208.
Xue, L.C., Rodrigues, J.P., Kastritis, P.L., Bonvin, A.M., Vangone, A., 2016. PRODIGY: a web server for predicting the binding affinity of protein–protein complexes. Bioinformatics 32, 3676–3678. https://doi.org/10.1093/bioinformatics/btw514.
Yan, R., Zhang, Y., Li, Y., Xia, L., Guo, Y., Zhou, Q., 2020. Structural basis for the recognition of SARS-CoV-2 by full-length human ACE2. Science (1979) 367, 1444–1448. https://doi.org/10.1126/science.abb2762.
Yang, T., Xu, C., 2017. Physiology and pathophysiology of the intrarenal renin-angiotensin system: an update. J. Am. Soc. Nephrol. 28, 1040–1049. https://doi.org/10.1681/ASN.2016070734.
Yang, J., Petitjean, S.J.L., Koehler, M., Zhang, Q., Dumitru, A.C., Chen, W., Derclaye, S., Vincent, S.P., Soumillion, P., Alsteens, D., 2020. Molecular interaction and inhibition of SARS-CoV-2 binding to the ACE2 receptor. Nat. Commun. 11, 4541. https://doi.org/10.1038/s41467-020-18319-6.
Yin, Y., Sheng, Y., Wang, M., Ma, Y., Ding, H., 2021. Interaction of serum proteins with SARS-CoV-2 RBD. Nanoscale 13, 12865–12873. https://doi.org/10.1039/D1NR02687A.
Zekri-Nechar, K., Zamorano-León, J.J., Reche, C., Giner, M., López-de-Andrés, A., Jiménez-García, R., López-Farré, A.J., Martínez-Martínez, C.H., 2022. Spike protein subunits of SARS-CoV-2 alter mitochondrial metabolism in human pulmonary microvascular endothelial cells: involvement of factor xa. Dis. Markers 1–11. https://doi.org/10.1155/2022/1118195, 2022.
Zerbato, V., Sanson, G., De Luca, M., Di Bella, S., di Masi, A., Caironi, P., Marini, B., Ippodrino, R., Luzzati, R., 2022. The impact of serum albumin levels on COVID-19 mortality. Infect. Dis. Rep. 14, 278–286. https://doi.org/10.3390/idr14030034.
Zhu, N., Zhang, D., Wang, W., Li, X., Yang, B., Song, J., Zhao, X., Huang, B., Shi, W., Lu, R., Niu, P., Zhan, F., Ma, X., Wang, D., Xu, W., Wu, G., Gao, G.F., Tan, W., 2020. A novel coronavirus from patients with pneumonia in China, 2019. N. Engl. J. Med. 382, 727–733. https://doi.org/10.1056/NEJMoa2001017.